Analyzing the Eyjafjallajökull 2010 eruption using satellite remote sensing, lidar and WRF-Chem dispersion and tracking model

P. W. Webley,[1,2] T. Steensen,[1,2] M. Stuefer,[1] G. Grell,[3] S. Freitas,[4] and M. Pavolonis[5]

Received 1 September 2011; revised 23 May 2012; accepted 27 May 2012; published 13 July 2012.

[1] Volcanic ash forecasting is a critical tool in hazard assessment and operational volcano monitoring. The use of volcanic ash transport and dispersion models allows analysts to determine the future location of ash clouds. In April–May 2010, Eyjafjallajökull in Iceland erupted explosively. Presented here is an evaluation of the volcanic application of the weather research and forecasting in-line chemistry model (WRF-Chem) applied to Eyjafjallajökull. The analysis focuses on the first few days of the explosive events, April 14–19. The model simulations are presented along with multiple satellite and ground based tools to compare and validate the results. The WRF-Chem results showed the ash cloud dispersing toward mainland Europe, with concentrations crossing Europe between 0.5–2.0 mg/m^3, centered at 5 km ASL, +/−1 km. Comparisons with satellite volcanic ash retrievals showed a good agreement and ground-based Light Detection And Ranging (LIDAR) data compared well to the model simulations. The analysis in this manuscript has illustrated the use of WRF-Chem for volcanic eruptions, with the coupled numerical weather simulation and ash forecasting important to understand the local atmospheric conditions as well as the ash cloud distribution. We show that to fully forecast ash concentrations, to the level of mg's per m^3, there is a need for accurate knowledge of the plume height; mass eruption rate; particle size distribution and duration along with a fusion of all data. Then accurate hazard assessments can be performed to limit the impact that dispersing clouds have on the aviation community and population.

Citation: Webley, P. W., T. Steensen, M. Stuefer, G. Grell, S. Freitas, and M. Pavolonis (2012), Analyzing the Eyjafjallajökull 2010 eruption using satellite remote sensing, lidar and WRF-Chem dispersion and tracking model, *J. Geophys. Res.*, *117*, D00U26, doi:10.1029/2011JD016817.

1. Introduction

[2] Volcanoes, when they erupt explosively, can generate gases as well as particulate matter, in the form of volcanic ash/tephra, sending them high into the atmosphere. Both volcanic sulfur dioxide and ash are hazards to local communities, regional districts, and countries, and can cause problems on a continental scale. The aviation community is concerned about the detection and tracking of volcanic ash clouds to provide hazard mitigation and timely warnings to any aircraft and airports. Volcanic Ash Advisory Centers (VAAC), set up by the International Civil Aviation Organization (ICAO), provide the information to the aviation community through timely volcanic ash advisories (VAA). Currently, operational detection of ash clouds uses satellite remote sensing data at VAAC's and volcano observatories alike [*Dean et al.*, 2004; *Webley et al.*, 2009a] and their future locations are provided using volcanic ash tracking and dispersion models (i.e., Numerical Atmospheric-dispersion Modeling Environment (NAME) [*Jones et al.*, 2007]; PUFF [*Searcy et al.*, 1998]; Hybrid Single-Particle Lagrangian Integrated Trajectory (HYSPLIT) [*Draxler and Hess*, 1998]; and Modèle Lagrangien de Dispersion de Particules d'ordre zéro (MLDP0) [*D'Amours and Malo*, 2004]. Validation of these model simulations is required so that the forecasts can be used to provide quantitative results on volcanic ash airborne concentrations.

[3] During any particular year, there are multiple volcanoes worldwide that have some type of large eruption (Volcano Explosivity Index (VEI) of 4 (see *Newhall and Self* [1982] for explanation of VEI)), be it *effusive* lava generating eruption or an *explosive* large ash plume and cloud-generating event. In March and April 2010, Eyjafjallajökull,

[1]Geophysical Institute, University of Alaska Fairbanks, Fairbanks, Alaska, USA.
[2]Alaska Volcano Observatory, University of Alaska Fairbanks, Fairbanks, Alaska, USA.
[3]Earth Systems Research Laboratory, National Oceanic and Atmospheric Administration, Boulder, Colorado, USA.
[4]Center for Weather Prediction and Climate Studies, INPE, São Paulo, Brazil.
[5]Center for Satellite Applications and Research, National Oceanic and Atmospheric Administration, Madison, Wisconsin, USA.

Corresponding author: P. Webley, Geophysical Institute, University of Alaska Fairbanks, 903 Koyukuk Dr., Fairbanks, AL 99775-7320, USA. (pwebley@gi.alaska.edu)

0148-0227/12/2011JD016817

Iceland produced both an effusive and explosive phase to its eruptive behavior [*Gudmundsson et al.*, 2010]. An earthquake swarm occurred between 23:00 UTC on April 13, 2010 and 01:00 UTC on April 14, 2010. This was followed by an initial ash loaded eruption plume that rose to more than 8 km above sea level (ASL) and was advected to the east by the local weather system.

[4] The analysis presented here will focus on the early part of the explosive phase from April 14–19, 2010 by performing a validation of volcanic ash transport and dispersion (VATD) model simulations. These model simulations are performed using a version of the Weather Research Forecast (WRF) [*Skamarock et al.*, 2005] model coupled with Chemistry (WRF-Chem) [*Grell et al.*, 2005]. Treatment of volcanic ash was recently included [*Freitas et al.*, 2011; M. Stuefer et al., Inclusion of ash and sulfur dioxide emissions from volcanic eruptions in WRF-Chem: Development and some applications, submitted to *Geoscientific Model Development*, 2012]. Validation is performed using thermal infrared satellite data from the Meteosat Second Generation (MSG) sensor Spinning Enhanced Visible Infra-Red Imager (SEVIRI) [*Steensen et al.*, 2012] as well as ground observations from Light Detection And Ranging (LIDAR) stations from across Europe. This study aims to (1) assess and validate WRF-Chem as an volcanic ash tracking and dispersion model and (2) discuss the operational capabilities to forecast volcanic ash concentrations in real-time.

2. Satellite Remote Sensing of Ash Clouds

[5] Remote sensing data provides a near-real time tool for detecting surface thermal activity and volcanic plumes and clouds as they disperse in the atmosphere. Volcanic gas and ash emissions are usually described as a either a plume (still attached to the summit) and as a cloud (detached and dispersed into the atmosphere). Ash clouds consist of a mixture of volcanic gas and silica-rich glass and can melt within aircraft turbine engines causing turbine failure [*Casadevall*, 1994]. Timely knowledge of the ash clouds location is critical for hazard mitigation therefore real-time volcano monitoring is critical to determine both impending and current volcanic activity.

[6] Satellite remote sensing has become a useful monitoring tool for detecting and tracking these potentially hazardous ash clouds [e.g., *Schneider et al.*, 1995; *Dean et al.*, 2004; *Bailey et al.*, 2010]. Thermal infrared (TIR) wavelengths have been used operationally for the detection and analysis of volcanic ash clouds such as *Webley et al.* [2009a]. Satellite data recorded from the thermal radiance measured at 10–12 μm wavelengths are sensitive to the temperature, optical depth, and effective particle radius of ash clouds. For the reverse absorption method [*Prata*, 1989a, 1989b] to be successful, some part of the ash cloud needs to be termed as 'semi-transparent', which indicates a low optical depth, generally less than 2.0. This technique uses the difference between the 11–12 μm from the 10–11 μm satellite data to give a brightness temperature difference (BTD). A negative difference between the two channels generally equates to an ash signal, made up of dry, fine-grained ash.

[7] For analysis of the 2010 volcanic clouds from Eyjafjallajökull, data from the SEVIRI sensor abroad the European Organization for the Exploitation of Meteorological Satellites (EUMETSAT) Meteosat-8 satellite was applied. This provided geosynchronous views, centered at 0°E, with 15-min intervals between data acquisition, across 3 visible and 8 infrared (at 3 × 3 km spatial resolution) channels and high-resolution visible channels (1 × 1 km) for providing false color imagery [*European Space Agency*, 2011]. Note that the spatial resolution is coarser closer to the poles for geosynchronous views. SEVIRI bands 9 (10.8 μm) and 10 (12 μm) were utilized to determine the spatial extent of the ash clouds based on thermal infrared (TIR) images. For the first four days from April 14–18, 2010, the ash clouds were detected through the BTD method across Europe using SEVIRI data snapshots every hour. Figure 1 shows a composite of SEVIRI data during this time period and emphasizes the cloud's location.

[8] Several methods exist to determine volcanic ash cloud properties from infrared radiances, such as *Wen and Rose* [1994], P*rata and Grant* [2001], and *Pavolonis and Sieglaff* [2010]. These methods utilize various forms of mathematical inversion to determine the total mass (kt); volcanic ash mass loadings (kg/m^2) within each satellite pixel; the effective radii (the ratio of the third moment to the second moment of the size distribution [see *Hansen and Travis*, 1974]; cloud optical depth;, and depending on the method, the ash cloud height from measured infrared radiances. Several assumptions are needed on cloud thickness to convert the satellite derived mass loading (kg/m^2) into a detectable concentration (kg/m^3).

3. Eyjafjallajökull, WRF-Chem and Ash Cloud Modeling

[9] Inter-comparisons between volcanic ash transport and dispersion models, volcanic ash real-time advisories as well as to the satellite observations have been reported by multiple authors, such as *Witham et al.* [2007], *Webley et al.* [2009b] and *Peterson et al.* [2012]. There are numerous volcanic ash transport and dispersion models available worldwide and recent efforts have occurred to compare them [*World Meteorological Organization* (*WMO*), 2010]. These models usually require that numerical weather prediction data be first generated and then the VATD model simulations use this data, either in a Lagrangian or Eulerian approach, to forecast the ash cloud movement. Some models run quickly such as PUFF [*Searcy et al.*, 1998] can run within minutes and others require many hours to run, such as ATHAM [*Oberhuber et al.*, 1998] requires several days. Note that *Oberhuber et al.* [1998] state it is not set-out to be an operational model. Other VATD models are used in operational settings, like NAME [see *Jones et al.*, 2007] and HYSPLIT [*Draxler and Hess*, 1998] and therefore are designed to produce volcanic ash simulations quickly for the corresponding volcanic ash advisory center.

3.1. WRF-Chem Model Details

[10] In our study, WRF-Chem is used, that employs an online approach. Online approaches should represent transport processes more accurately and allow for feedback to meteorology [*Grell and Baklanov*, 2011]. However, in the simulations shown here for Eyjafjallajökull, this feature is not used. An assessment of the feedback versus tracer

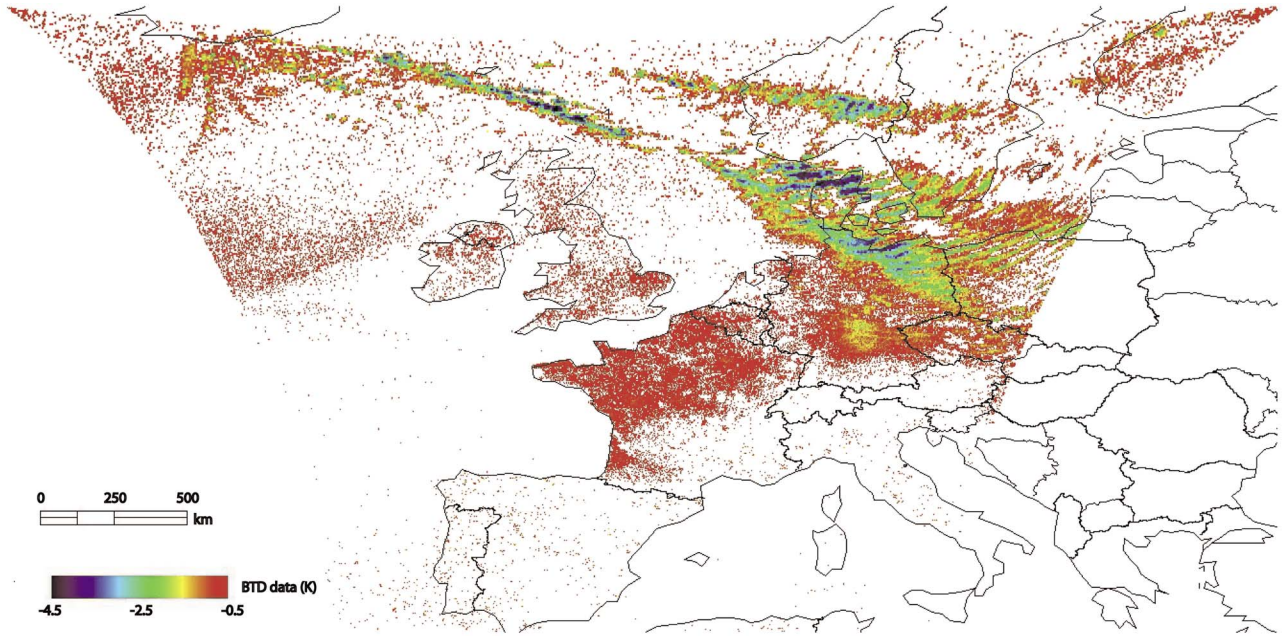

Figure 1. Volcanic ash brightness temperature difference (BTD) composite map, showing minimum ash reverse absorption signal during April 14–18, 2010. This is a composite of the negative BTD data per hour imagery. Each image is compared to the composite and if negative BTD is stronger (more negative) than the composite, then data in the composite at that pixel is substituted with the more negative data. Hence, the final composite shows the full track of the ash cloud, but does include substantial noise from non-volcanic cloud features. It provides an overview of the ash's movement across Europe.

approach is beyond the study here. Additional computational costs compared to a meteorology only run are small compared to full chemistry runs, and depend on the number of additional prognostic variables (10 for our experiments). We use the model in a tracer mode to be able to produce volcanic ash simulations in a timely and useful manner for operational forecasting.

[11] The WRF-Chem design used for the Eyjafjallajökull events uses a 18 km spatial resolution, with 36 vertical levels and 10 volcanic ash bins. Using 96 CPU-cores (where there is up to 4 GB of memory is available per core and CPU speeds between 2.2–2.3 GHz), a 60 times speed up is accomplished, i.e., 24 h simulations takes approximately 24 min. This is over a domain of 300 $\times$ 200 grid points. When compared to a numerical weather prediction WRF only run, i.e., no volcanic ash bins, WRF-Chem would take 50% longer on a single processor, which would reduce further in the parallel mode. Here in this study, the model is used with no feedback and the ash concentrations are advected and diffused throughout the model domain by three-dimensional numerical weather prediction wind fields. Our model domain and spatial resolution was designed to allow model outputs to be generated within the time window for operation processing. A follow-up paper is in progress to study the effects of volcanic ash from Eyjafjallajökull on clouds and radiation using much more involved and computationally expensive chemical modules.

[12] Recent developments with WRF-Chem include the implementation of an initial volcanic plume model [*Freitas et al.*, 2011]. Large explosive volcanic plumes have a typical 'umbrella' shaped vertical distribution (detailed in *Sparks et al.* [1997]) and as such this distribution is adapted into WRF-Chem. Further work is required to develop additional vertical structure types. A volcanic plume module generates the source data for WRF-Chem [*Freitas et al.*, 2011]. The necessary input parameters include the erupted mass, the initial altitudes of the ash plume, an eruption rate, and an ash grain size distribution. *Mastin et al.* [2009] 'Eruption Source Parameters (ESP)' for the world's volcanoes are used by the *Freitas et al.* [2011] module as a look up table. WRF-Chem through the add-on initial plume module uses the ESP type data as volcanic emission information for the model forecasting. Output data are directly readable by model routines to generate volcanic ash initialization and boundary conditions for the forecast.

3.2. Model Simulation Initialization

[13] WRF-Chem simulations of the April period of activity from Eyjafjallajökull used the local weather radar station (Icelandic Meteorological Office, Eyjafjallajökull 2010 plume altitude measured by weather radar, http://andvari.vedur.is/~arason/radar/, viewed April 16, 2011) (hereinafter IMO, online data, 2010) for actual plume altitudes from the eruptive period (Table 1) and defined particle size distribution from ESP data (Table 2). Additional initialization parameters are defined in the ESP type S2, as defined by *Mastin et al.* [2009]. The initial eruption column is represented as an 'umbrella' vertical mass distribution within the closest pixel to the volcanoes location. The umbrella vertical mass distribution is defined by the height of the base of the umbrella. This base was set at 27% of the maximum height; so a 9 km plume ASL would have a 2.5 km deep umbrella portion. Within the umbrella, a Gaussian distribution is defined, so the peak of the distribution is within the middle

Table 1. Weather Research Forecast Coupled With Chemistry (WRF-Chem) Model Simulation Input Parameters for April 14–19, 2010 Period of Activity at Eyjafjallajökull[a]

Start Time (UTC)	Duration (h)	End Time	Height ASL (km)	Eruption Rate (m^3/s)	Eruption Rate (kg/s)	Total Mass (kg)
4/14/2010 09:00	10	4/14/2010 19:00	9	219.553	5.71E+05	2.06E+10
4/14/2010 19:00	9	4/15/2010 04:00	5.5	14.884	3.87E+04	1.25E+09
4/15/2010 04:00	39	4/16/2010 19:00	6	119.503	6.44E+04	9.04E+09
4/16/2010 19:00	35	4/18/2010 06:00	8.25	140.325	3.65E+05	4.60E+10
4/18/2010 06:00	17	4/18/2010 23:00	5	8.335	2.17E+04	1.33E+09
4/18/2010 23:00	1	4/19/2010 00:00	4	1.898	4.93E+03	1.78E+07

[a]Total mass as determined from *Mastin et al.* [2009] relationship between plume height above vent and total volume and plume altitude from the Icelandic Meteorological Office (IMO) radar data (IMO online data, 2010). Umbrella cloud (defined by Poisson distribution), 18 km spatial resolution and particle size distributions as defined in Table 2. Dates are given as month/day/year.

of the umbrella. This produces approximately 80% of the total mass in the vertical is included in the umbrella and 20% is then uniformly distributed below the umbrella portion. This is similar to the defined vertical mass distribution used by the PUFF VATD model [*Peterson*, 2006, page 22]. This is not the ideal plume distribution for the events from Eyjafjallajökull and further work on the plume model will aim to develop multiple options for the vertical structure to allow uniform, exponential with height and other detailed approaches of *Carey* [1986] and *Suzuki* [1983]. The time series of radar data from IMO (online data, 2010) provided an unprecedented level of detail for the initial plume height, Figure 2. For the WRF-Chem simulations, the plume altitude was defined for the different periods of the eruption, illustrated in Figure 2. This provided an approximation of the measured plume heights from radar on an hourly basis, without needing to re-initialize the model every 5 min.

[14] To determine the total mass (kg) from the eruption duration and the mass eruption rate (kg/s), an empirical relationship approach of *Sparks et al.* [1997] and *Mastin et al.* [2009] was chosen. This approach relates eruption rate (kg/s) from a measured plume height using past volcanic events. With known eruption duration (seconds) and the empirical relationship, the total mass (kg) for our WRF-Chem simulations was determined using the *Mastin et al.* [2009] approach. Table 1 shows the calculated eruption rates (kg/s) and total mass (kg) for each of the periods of differing plume heights. Figure 2 shows that for April 16–17, 2010 the maximum plume height was around 8 km ASL. Additionally, during this time period, it was at 4.5–5 km ASL. During this period, the plume height was between 4.5–5.5 km ASL for 66% of the time and between 8–8.5 km ASL for 24% of the time. Using the 5.5 km ASL for the initial altitude would be an underestimate for 34% of time. Using a plume height of 8–8.5 km would be overestimate for 76% of time.

[15] However, usually during an event one does not have this level of temporal periodicity and in most cases volcano observatories and volcanic ash advisory centers use the maximum recorded height and then determine the eruption rate from this observation. We have simplified the data to use a common initial plume height from the radar data, rather than a variable source height and mass per hour. For certain volcanic events, satellite remote sensing might not be able to detect any plume for hours between satellite measurements. Hence, we used the 8.5 km ASL observations as a worst-case-scenario.

[16] The WRF-Chem model simulations used here for Eyjafjallajökull use the S2 type of *Mastin et al.* [2009]. They state that for this type, 40% of the initial ash mass distribution is for particles less than 63 μm in diameter, and therefore 60% of the initial ash mass for coarser particles. WRF-Chem requires a full size distribution within defined particle bins. *Mastin et al.* [2009] provide details of the eruption used for the S2 type and the reference therein for the ash particle size distribution. For the S2 type, this is *Durant and Rose* [2009]. Their analysis of the Crater Peak, Mount Spurr event from 1992 provides the base for the S2 type particle size distribution. Hence, Table 2 provides the ash distribution from their analysis and is used by WRF-Chem for its 10 volcanic ash bins. For each *Mastin et al.* [2009] type, a complete size distribution has been obtained for all 10 volcanic ash bins and added to the initial plume module of *Freitas et al.* [2011] used in the model initialization.

[17] Table 2 provides details of the particle size distribution used by WRF-Chem for the S2 type. For particle sizes greater than 1 mm (WRF-Chem ash bin 1 and coarser), all particles are loaded into the 1–2 mm ash bin. There are particles greater than 2 mm in size in the *Durant and Rose* [2009] samples. To include the total mass distribution within the model run, we have included them all in the coarsest ash bin (1–2 mm). This means a higher mass fraction has been allocated in this bin and an under-representation of the mass fractions for the large particles (>2 mm). Including particles larger than 2 mm in the 1–2 mm size bin would not affect the modeled ash cloud over Europe as these particles fall out quickly, but would be significant for ashfall simulations, that we do not analysis in his study.

[18] The National Centers for Environmental Prediction (NCEP) Final (FNL) Operational Global Analysis data were

Table 2. Volcanic Ash Size Particle Distribution for Weather Research Forecast Coupled With Chemistry (WRF-Chem) Model Simulations During the April 14–19, 2010 Events From Eyjafjallajökull Using Eruption Source Parameter (ESP) Types S2[a]

Bin	Particle Diameter Within Bin	Phi Size	Percent of Mass S2
1	1 to 2 mm	−1 to 0	22
2	0.5 to 1 mm	0 to 1	5
3	0.25 to 5 mm	1 to 2	4
4	125 to 250 μm	2 to 3	5
5	62.5 to 125 μm	3 to 4	24.5
6	31.25 to 62.5 μm	4 to 5	12
7	15.625 to 31.25 μm	5 to 6	11
8	7.8125 to 15.625 μm	6 to 7	8
9	3.9065 to 7.8125 μm	7 to 8	5
10	<3.9 μm	>8	3.5

[a]WRF-Chem array bin defined for model-satellite and model-ground observations analysis.

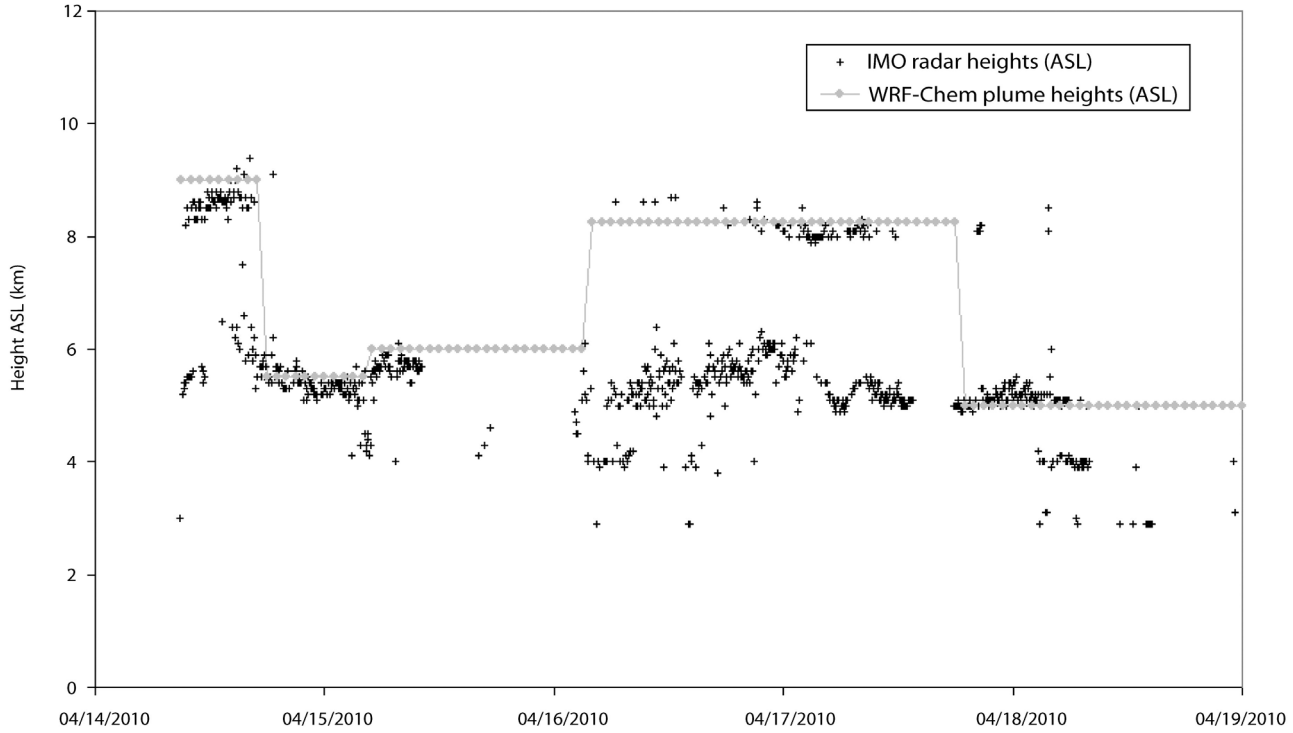

Figure 2. Comparison of IMO radar heights and Weather Research Forecast coupled with Chemistry (WRF-Chem) plume heights above sea level.

used to provide initial and boundary meteorological conditions for the WRF-Chem runs (http://dss.ucar.edu/datasets/ds083.2/). A 5-day WRF simulation starting at 0000 UTC, 14 April 2010 was performed. The modeling domain extended over 300 × 200 grid cells with a spatial resolution of 18 km; 36 pressure-based stretched vertical levels were chosen for this study, varying in thickness from a few hundred meters at surface to 1 km at the model top, up to 20 km ASL. The Weather Research and Forecasting (WRF) model includes various options for dynamic cores and physical parameterizations [*Skamarock et al.*, 2005] so that it can be used to simulate atmospheric processes over a wide range of spatial and temporal scales. WRF-Chem, the chemistry version of the WRF model [*Grell et al.*, 2005], simulates trace gases and particulates interactively with the meteorological fields.

[19] The volcanic ash concentrations are treated as tracers within the WRF-Chem simulations ran for this case study. As the ash is transported within the Eulerian modeling environment, the ash concentrations per grid box are impacted by resolved (advection) and unresolved (diffusion, turbulence, convection) transport, settling, and wet deposition. More details on the different resolved and unresolved transport schemes, types of ash deposition and on the mentioned parameterization schemes can be found in Stuefer et al. (submitted manuscript, 2012). In this manuscript, we are focusing on the application of WRF-Chem to a volcanic ash event.

3.3. Model Run Results

[20] WRF-Chem simulations showed that early on (April 14, 2010 at 12:00 UTC, Figure 3a) wind patterns advected the modeled ash cloud to the northeast of Iceland. This closely matches the VAAC forecast also from 12:00 UTC (Figure 4a). By 00:00 UTC on April 15, 2010 the modeled ash cloud's main trajectory turned to be southeasterly toward mainland North-Western Europe and the United Kingdom (Figure 3b). Again, the WRF-Chem simulations matched well with the VAAC advisory (Figure 4a). This southeasterly advection of the ash cloud during April 15, 2010 and until April 16, 2010 at 00:00 UTC (Figure 3c), when the modeled ash cloud is advected toward mainland Europe. This simulation shows a good agreement to the modeling approach of *Ansmann et al.* [2011] with the regional atmospheric transport model, Chemistry-Transport Model System (COSMO-MUSCAT) and *Chazette et al.* [2012] with the Eulerian Polair3D chemistry and transport model. The VAAC volcanic ash advisories (VAA), generated operationally at the time of the eruption, are a good match to the WRF-Chem model simulations. Both the VAA's (Figure 4) showed ash being forecasted across mainland Europe as well as significant surface to FL200 (approximately but not directly equated to 20,000 feet above sea level as flight levels are on a pressure based coordinate system) ash across the United Kingdom (Figure 4b). Note that the VAA's are ash cloud locations at set altitude bounds and the WRF-Chem ash cloud simulations are for the full column as a mass loading. Comparison of the full extent of all three levels in the VAA with the mass loading from the WRF-Chem model provides a good match, showing that the model simulations used in the VAA, from the NAME model, match well to WRF-Chem.

[21] The ash mass loadings from our simulations, represent all the volcanic ash mass from volcanic ash particle size bin 1 (1 to 2 mm diameter) to volcanic ash bin 10 (less than 3.9 μm). Note that with any volcanic ash model simulation,

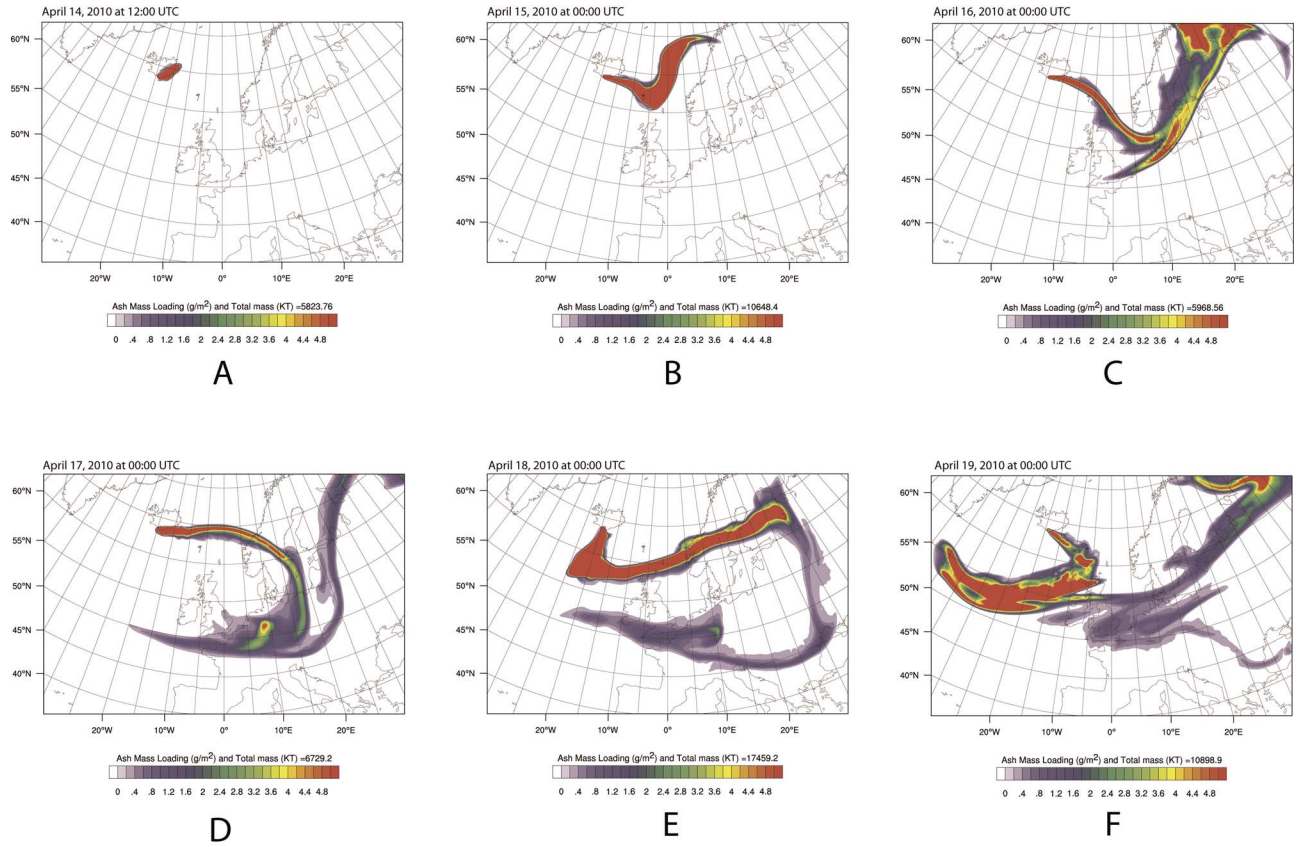

Figure 3. Time snapshots from Weather Research Forecast coupled with Chemistry (WRF-Chem) model simulation of April 14–19, 2010 volcanic ash clouds from Eyjafjallajökull volcano at (a) 12:00 UTC on April 14, (b) 00:00 UTC on April 15, (c) 00:00 UTC on April 16, (d) 00:00 UTC on April 17, (e) 00:00 UTC on April 18 and (f) 00:00 UTC on April 19, 2010.

the initial size distribution and associated mass is critical in terms of influencing the downwind ash concentrations. More fine ash (<63 μm) initially will lead to greater downwind concentrations and vice versa for more coarse ash (>63 μm), which will fall out quicker and influence any ashfall model results. The model simulated the three-dimensional dispersion and transport of the volcanic ash cloud from Eyjafjallajökull. Therefore, analysis of the ash concentrations and mass loading per ash particle bin will determine which ash bin dominated the transport. Analysis of the model outputs

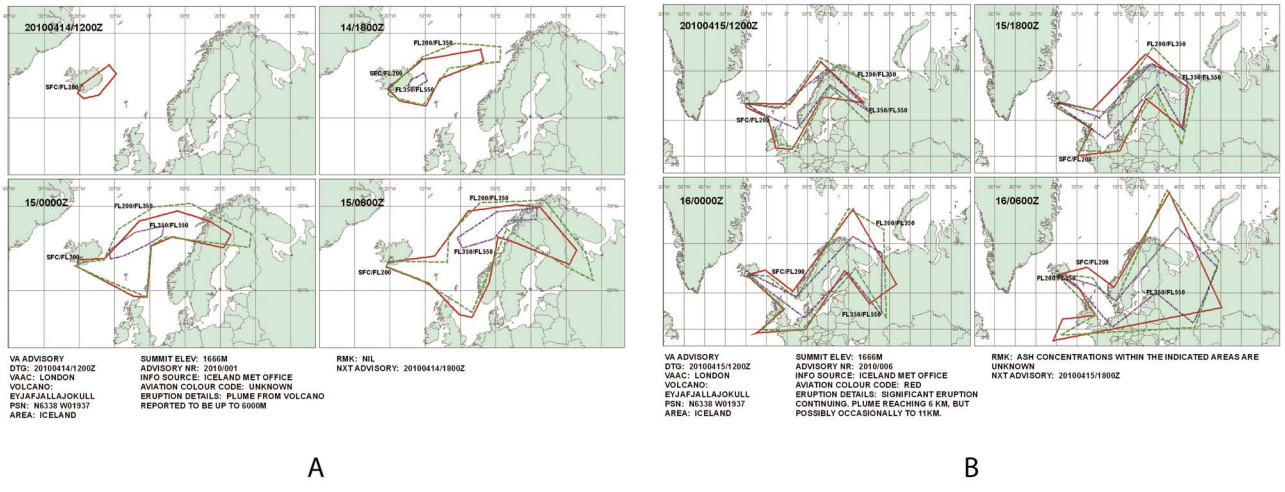

Figure 4. (a) Volcanic Ash Advisory Center (VAAC) forecast at 12:00 Z (UTC) forecast on April 14 until April 15, 2010 at 06:00 Z (UTC) and (b) VAAC forecast at 12:00 Z (UTC) forecast on April 15 until April 16, 2010 at 06:00 Z (UTC). Imagery courtesy of the London VAAC.

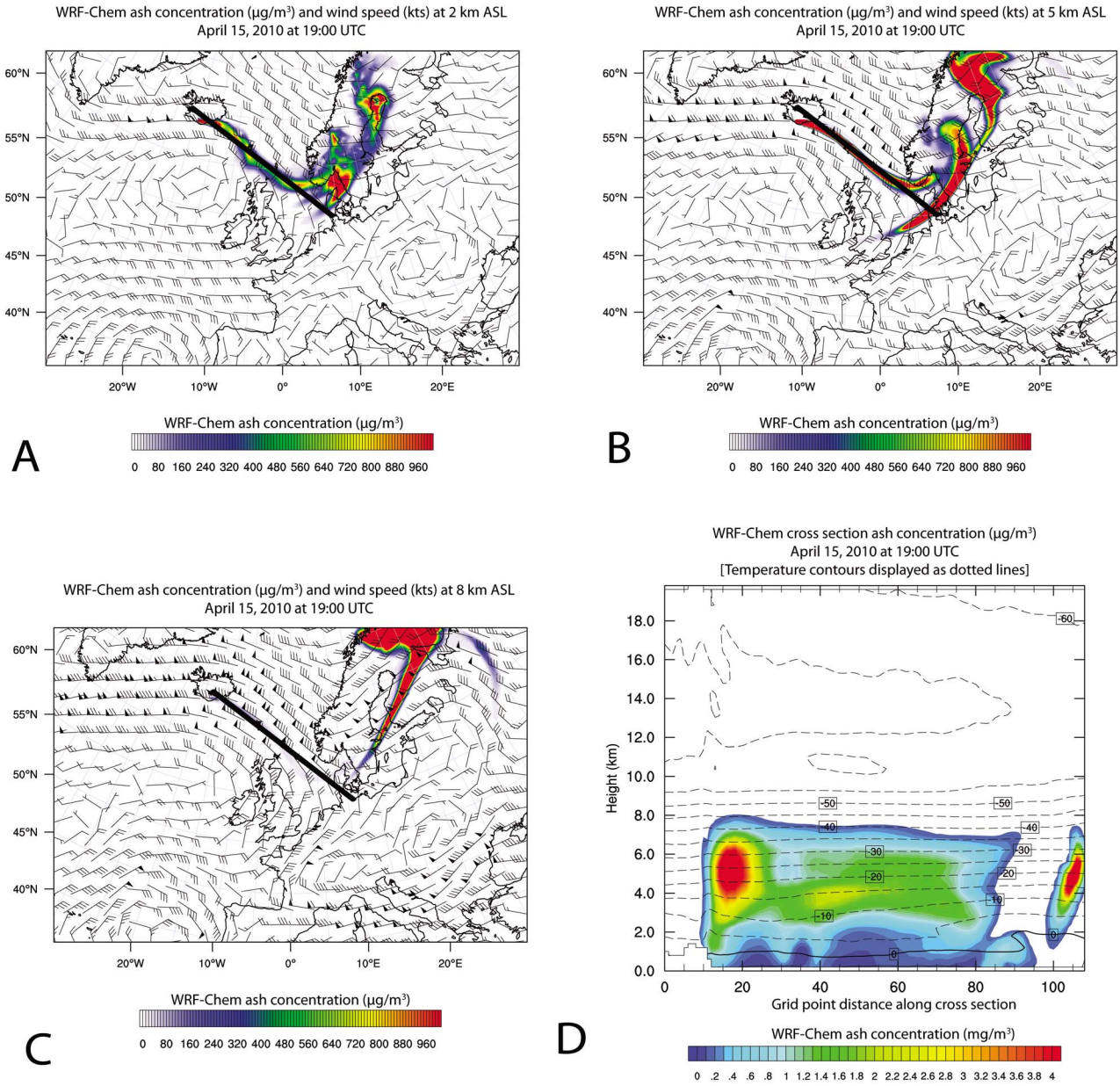

Figure 5. Weather Research Forecast coupled with Chemistry (WRF-Chem) modeled volcanic ash concentrations at defined altitudes of (a) 2, (b) 5 and (c) 8 km above sea level; (d) vertical slice through the atmosphere along defined cross section on April 15, 2010 at 19:00 UTC. Black line in (Figures 5a–5c) represents cross section location (Figure 5d).

showed that all of the volcanic mass within the ash bins from bin 1 (1 to 2 mm) to bin 5 (62.5 to 125 μm) were not advected beyond 120 km from the volcano. *Schneider et al.* [1999] showed particles of 50 μm in size will have residence time of less than 5 h given spherical particles falling out of a 20 km ASL initial plume and *Rose et al.* [2001] state that within Stage 1, 0–12 h after emission, there will be rapid fallout of particles greater than 500 μm in size (WRF-Chem bins 1, 2 and 3) within 25 km of the volcano. Note this is for settling without account for lofting due to atmospheric conditions. These two studies illustrate that the larger ash particles will fall out in close proximity to the volcano. However, it does approximate the potential distances a particle will travel from a volcano. So, it is likely volcanic ash concentrations for the simulated cloud many hundreds of kilometers downwind will mainly consist of ash from WRF-Chem bins 6, 7, 8, 9 and 10 (see Table 2 for size description).

[22] To examine the three-dimensional ash distribution and discuss the particle size distribution that is advected, two time snapshots have been chosen, Figure 5. The wind vector streamlines patterns at 00:00 UTC from April 16 and 18, 2010 and volcanic ash concentrations showed the dominant wind direction from the volcano was blowing toward the southeast and that the modeled ash cloud was then dispersed along streamlines so it was elongated in a southwest to

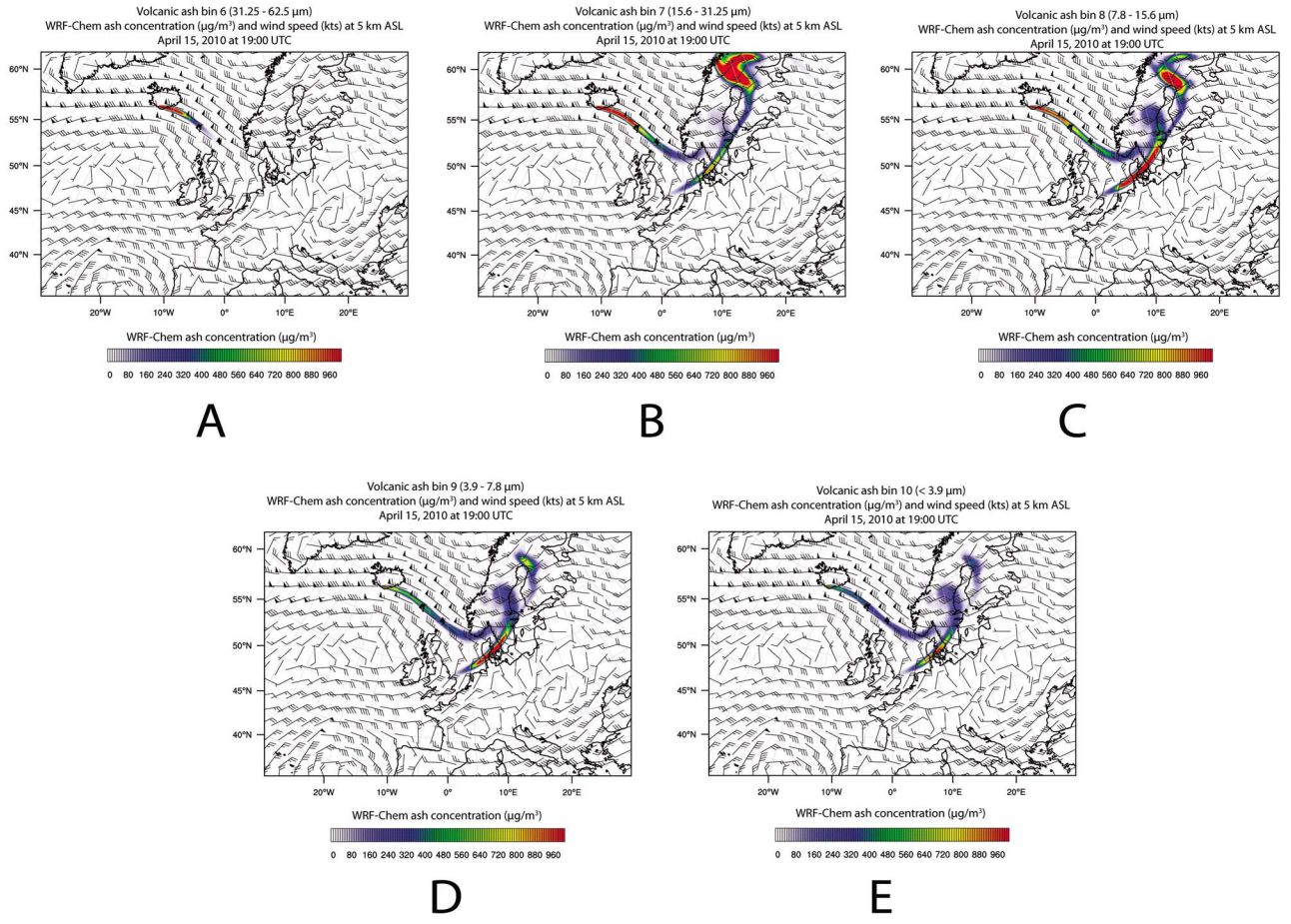

Figure 6. Weather Research Forecast coupled with Chemistry (WRF-Chem) modeled volcanic ash concentrations at 5 km above sea level on April 15, 2010 at 09:00 UTC. (a) Ash bin 6, (b) ash bin 7, (c) ash bin 8, (d) ash bin 9 and (e) ash bin 10.

northeast direction. The modeled ash cloud was then advected across mainland Europe with this elongated form. Examining modeled ash at different altitudes, Figure 5a to Figure 5c, shows how, although there were some variations in wind direction, the dominant flow direction was southeasterly toward mainland Europe. Higher altitude modeled ash was advected more northeasterly, Figure 5c, than at lower altitude of 2 and 5 km ASL, Figure 5a and Figure 5b. However, as the modeled cloud was advected further from the volcano, ash at all altitudes was advected in a southeasterly direction, while also been stretched along streamlines in a southwest to northeast direction.

[23] Examination of the modeled volcanic ash concentrations at 2 km ASL (Figure 5a) showed that by April 15, 2010 at 19:00 UTC, low altitude ash had reached Denmark and Northern Germany, with concentrations around 1000 $\mu g/m^3$. At higher altitudes, 5 km ASL (Figure 5b), modeled concentrations were greater than 1000 $\mu g/m^3$ and a more defined ash cloud existed. Modeled ash from WRF-Chem at 8 km ASL, was confined over northeast Scandinavia (Figure 5c). This was the remaining ash from the 8.5 km ASL plume on April 14/15 2010 that was initiated into WRF-Chem.

[24] In addition to the horizontal slices through the modeled volcanic ash cloud, vertical slices (Figure 5d) showed how the modeled ash cloud was not confined to one thin layer in the vertical. Note that this is heavily dependent on the initial vertical distribution, defined here for Eyjafjallajökull as uniform below the umbrella portion. Sensitivity of the downwind three dimensional shape to the initial vertical distribution was not conducted here and would require further study. The ash cloud's shape and distribution downwind is also very dependent on the atmospheric structure and with lack of vertical wind shear then the cloud would not develop into thin layers. Modeled concentrations greater than 2 mg/m^3 were generally confined close to the volcano and in small pockets downwind at 4 km ASL, Figure 5d. This modeled volcanic ash cloud passed across Northern Europe and was the dominant feature that matches to the observed volcanic ash BTD from the SEVIRI data (Figure 1).

[25] Volcanic ash concentration maps from each individual bin show that the ash particles from bins 7 and 8 in general dominated the dispersing cloud (Figure 6). Volcanic ash particles from the earlier erupting plume with sizes of 31.25–62.5 μm in diameter (Figure 6a) had settled out by 09:00 UTC on April 15, 2010. The concentrations of volcanic ash <7.8 μm in diameter (Figure 6d and Figure 6e) showed that these modeled volcanic ash particles propagated across Northern Europe (Northern Scandinavia), but the concentrations were lower than for the modeled concentrations with volcanic ash particles from 7.8–31.25 μm

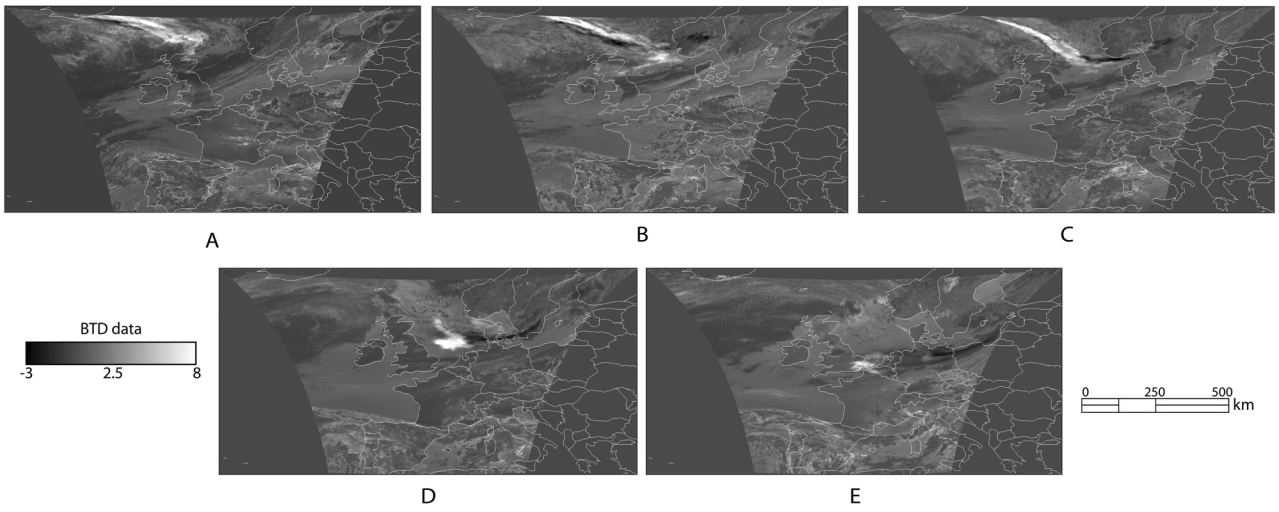

Figure 7. Spinning Enhanced Visible Infra-Red Imager (SEVIRI) brightness temperature difference maps for (a) 08:00 UTC, (b) 15:00 UTC and (c) 19:00 UTC on April 15, 2010 and (d) 01:00 UTC and (e) 08:00 UTC on April 16, 2010, scaled from +8 to −3 K.

(Figure 6b and Figure 6c). Again, the relative concentrations downwind of ash particle size bin 8 to 9 or 9 to 10 is dependent on their initial distribution as these sizes and their concentrations will only settle out very slowly and will therefore stay airborne for a significant time and downwind distance. Note that the BTD method for satellite thermal infrared data is most sensitive to volcanic ash clouds that have effective radii in the 5–10 μm range [*Wen and Rose*, 1994], or from the WRF-Chem simulation, where the volcanic ash bins 7 and 8 will dominate (7.8–31.25 μm), with smaller contributions from bins 6 (31.25–62.5 μm) and 9 (3.9–7.8 μm). Therefore, in Figure 1 when the BTD signal is detected, the ash cloud will be dominated by these ash particles.

[26] The effective radii is a measure of the skewness of the size distribution relative to the variance. In volcanic ash retrievals, this is assumed to be a lognormal distribution across a size range from 0.1 to 100 microns within that size distribution. The maximum value of the effective particle radius that can reliably be retrieved is about 15 μm. However, particles larger than 15 μm still do contribute to the measured radiation. All this means is that the largest value of the ratio of the third and second moments of the size distribution that can be retrieved is 15 μm Therefore, volcanic ash particles greater than 15 microns will be still airborne and if dominate then it will raise the retrieved effective radii until it 'saturates' at 15 μm. Large ash particles have similar emissivities at the wavelengths used in the reverse absorption method. Thus, when larger particles dominate, the reverse absorption signal can be very similar to the signal exhibited by certain liquid water and ice clouds. See *Prata* [1989a, 1989b], *Wen and Rose* [1994] and *Webley et al.* [2009a] for more on volcanic ash cloud detection, BTD method and when and where the method can be useful.

[27] Examination of height slices and cross sections through the WRF-Chem simulations shows that it is not a simple case of defined volcanic ash boundaries at a zero threshold; volcanic ash concentrations vary considerably through the atmosphere (Figure 5) and the airborne modeled concentrations are dominated by different particle size distributions (Figure 6) and are heavily dependent on the initial size distribution and vertical plume shape. As the majority of the modeled volcanic ash with particle sizes greater than 31.25 μm would fall out under gravitational settling within several hundred km of the volcano, the only modeled airborne ash that propagated across Europe as simulated by WRF-Chem was from bins 7 to 10, as defined in Table 2. Particle aggregation downwind of the volcano could result in 'larger' particles being measured, as seen in *Madonna et al.* [2010]. Such a process of aggregation is not included in WRF-Chem and hence finer particles would be modeled as the dominant sizes. Estimates of the total mass of ash from satellite-based BTD mapping may be underestimated since the sensitivity to effective radius decreases significantly when the effective radius exceeds 10 μm [*Pavolonis and Sieglaff*, 2010], resulting in an underestimate of the number of larger particles. Therefore, it is best to utilize satellite observations and ash cloud modeling in tandem for volcanic ash hazard assessment.

4. Volcanic Ash Retrievals From TIR Data

[28] SEVIRI TIR satellite data has been used to detect the volcanic ash cloud from the April 2010 activity at Eyjafjallajökull. The results shown here compare well with the approaches of *Francis et al.* [2012] and *Prata and Prata* [2012], whom both use the TIR satellite data to obtain the physical characteristics of the ash clouds, its mass loading, altitude, effective particle radii and optical depth. Fine, dry ash will provide a negative BTD signal between the TIR channels. Examining the BTD signal from +8 to −3 K (Figure 7) showed that there was a clear negative BTD signal across Europe, indicative of fine, dry ash, but also a positive signal collocated with this region, that was advected toward the United Kingdom by April 16, 2010 at 01:00 UTC (Figure 7d). This positive BTD signal could have been from water rich cloud or from ice coated volcanic ash. *Rose et al.* [2003] state that ice can cause a BTD to be positive, even

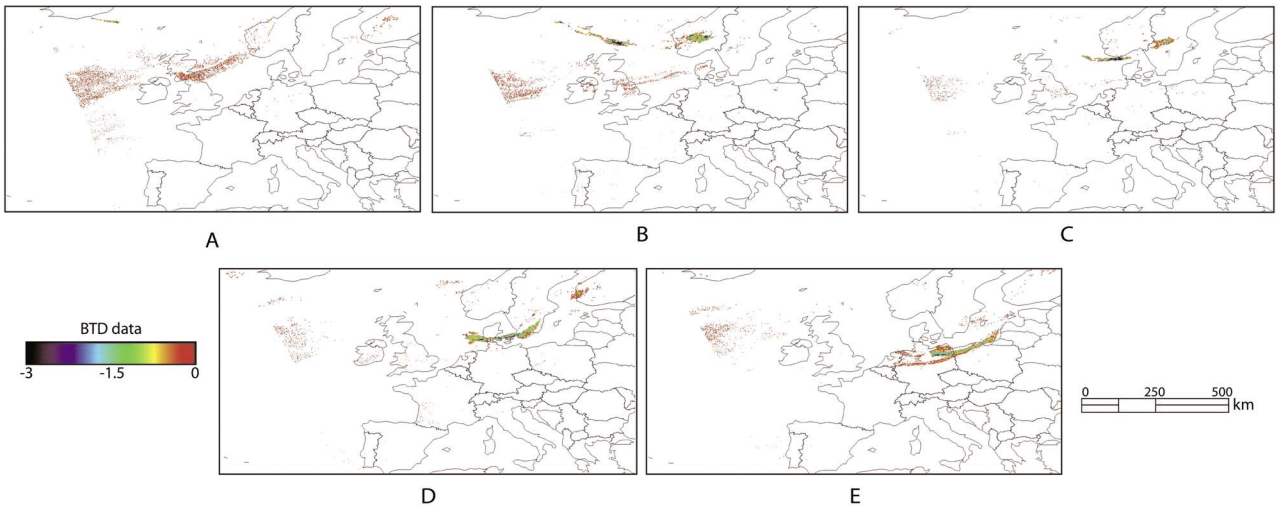

Figure 8. Spinning Enhanced Visible Infra-Red Imager (SEVIRI) brightness temperature difference maps for (a) 08:00 UTC, (b) 15:00 UTC and (c) 19:00 UTC on April 15, 2010 and (d) 01:00 UTC and (e) 08:00 UTC on April 16, 2010, scaled from 0 to −3 K.

when ash is present. *Dacre et al.* [2011] and *Devenish et al.* [2012] showed that volcanic ash was present, in low concentrations, across United Kingdom at the time of satellite data detected a positive BTD signal. Examination of just the negative BTD signal would show no detectable 'ash' over UK (see Figure 8). With the ground observations detecting there were low ash concentrations [*Dacre et al.*, 2011; *Devenish et al.*, 2012], and Figure 7b showing that the positive signal was coupled to the negative BTD at 15:00 UTC on April 15, 2010 and de-coupled by 08:00 UTC on April 16, 2010, then it is possible that the signal passing across the UK is volcanological, but rich in water, as compared to the dry, ash detected in the negative BTD across mainland Europe. Further analysis of the ash samples from the UK compared to those from mainland Europe is required to determine water content of the ash passing over the UK.

[29] Analysis of the negative BTD signal (Figure 8) showed a weak signal at the volcano on April 15, 2010 at 08:00 UTC (Figure 8a) that by 15:00 UTC (Figure 8b) and again by 19:00 UTC (Figure 8c) had tracked across the Northern Atlantic to mainland Europe. At 01:00 UTC (Figure 8d) and 08:00 UTC (Figure 8e) on April 16, 2010 there was a clear BTD signal over Europe. As the ash cloud passed across Eastern Europe, the BTD signal dropped below the detectable limits of the sensors and the method. With SEVIRI onboard a geosynchronous satellite system, then it has differing pixel resolutions from 3 km at the sub-satellite point to 10s of km closer to the poles. As the ash cloud dispersed, the TIR signal per pixel will drop as the optical depth of the ash cloud decreases and/or the temperature of the ash cloud approaches the background radiative temperature. Once this occurs, the BTD analysis will show no 'ash' signal as the concentration/mass loading is below the minimum detectable by the sensor and/or thermal contrast between the ash cloud and the background decreases. *International Volcanic Ash Task Force* (*IVATF*) [2011] determined that concentrations of 2 mg/m^3 for 1 km cloud or ash loading of 2 mg/m^2 can be reliably detected using infrared measurements and, again, ash is the highest cloud layer.

[30] The analysis of the volcanic ash mass loading and total mass within the ash cloud at defined time snapshots does not fully represent the full ash mass as it passed over Europe. Volcanic ash retrievals have to assume the particle size distribution within the atmosphere and as such may not resolve the full mass within the vertical column, (e.g., the number of larger particles may be underestimated). Time series for the total mass, mean effective radii, mean optical depth and total number of SEVIRI pixels in BTD analysis (Figure 9) illustrated the variation with time of the total mass and increase in size of the ash cloud. On those SEVIRI pixels flagged as a negative BTD using the reverse absorption method, the Volcanic Ash Retrieval (VAR) was performed, adapted from *Wen and Rose* [1994]. The VAR calculates masses, effective pixel radii and the optical depth of volcanic clouds. This retrieval is based on different assumptions including a spherical particle and a thin, homogenous cloud parallel to the surface. Here, a BTD threshold of −1 K was used to determine the SEVIRI data for the volcanic ash retrieval. Figure 10 showed that BTD signals from 0 to −3 K were evident across the SEVIRI footprint. Inclusion of the ash signal from 0 to −1 K in the retrieval would have weighted the results with nonvolcanic retrievals. *Webley et al.* [2009a] showed that other atmospheric conditions can lead to negative BTD signal between 0 and −1 K. Unless more detailed and complex retrievals such as those from *Pavolonis* [2010] and *Pavolonis and Sieglaff* [2010] are applied, weaker but potentially volcanic and/or nonvolcanic features have been eliminated from the VAR analysis.

[31] The total mass (Figure 9a) showed the increase in detected volcanic ash using the BTD data. Here, a cloud top temperature of 225 K, surface temperature of 280 K and cut off of −1.0 K were used in the VAR analysis. The initial increase in total mass to around 40 kT on April 15, 2010 at 15:00 UTC showed the growing cloud as it was advected from Iceland toward mainland Europe. The drop in ash mass

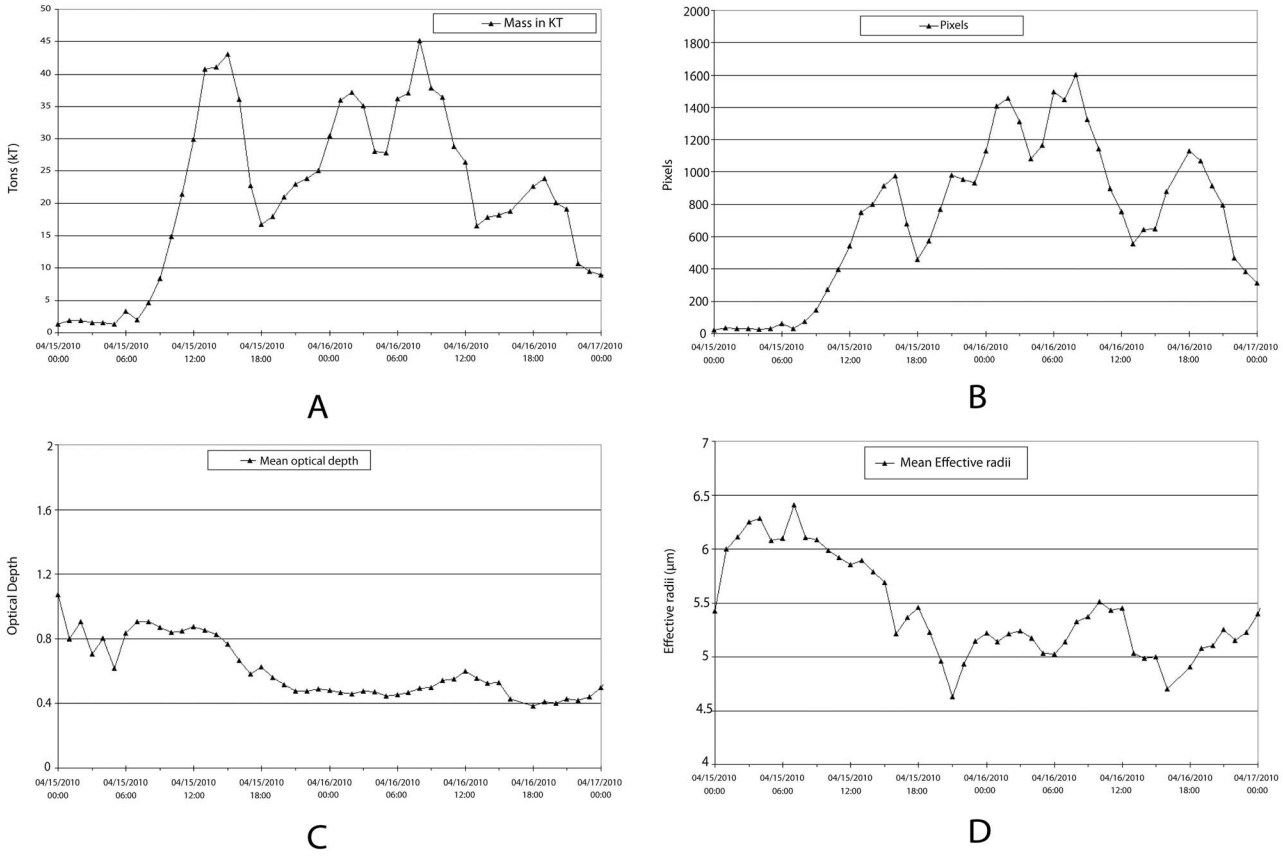

Figure 9. Volcanic ash retrievals for (a) Total mass (kT), (b) mean effective radii, (c) mean optical depth and (d) number of pixels within retrieval from April 15–17, 2010.

by 18:00 UTC on April 15 resulted from the ash signal that was advected toward Scandinavia either (1) passing below the detection threshold of the TIR retrieval; (2) not being the highest cloud layer; or (3) passing into a water rich atmosphere. All these factors will reduce the ability to detect the ash cloud with the BTD method. There was an increase in the ash mass until April 16 at 08:00 UTC from the ash cloud within the North Sea passing across Europe. The

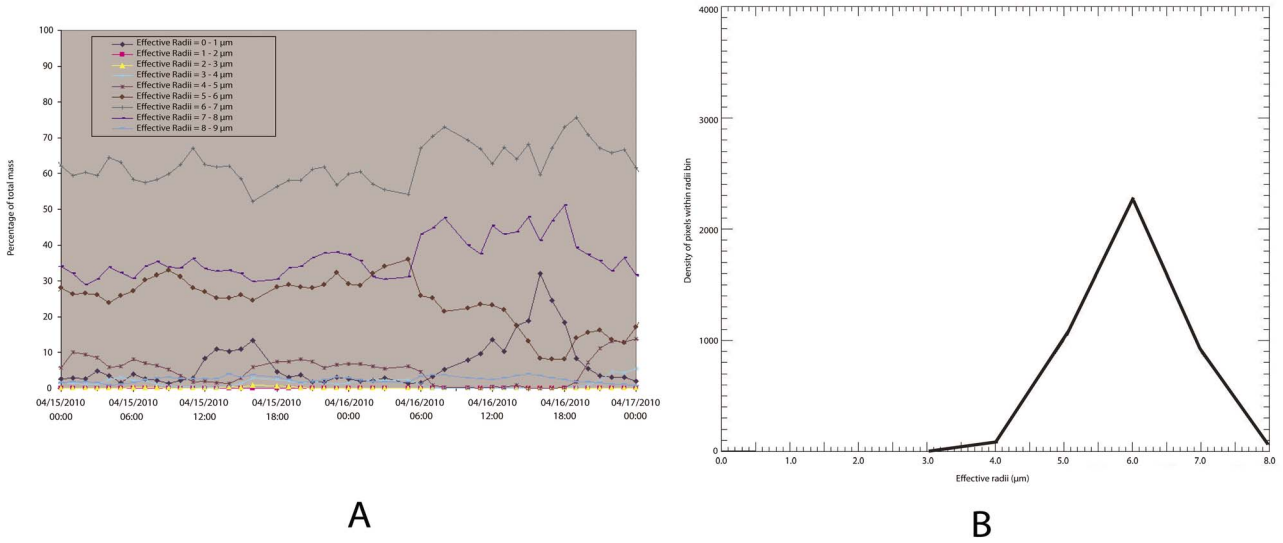

Figure 10. (a) Percentage of total mass per effective radii bins for volcanic ash retrievals from April 15–16 and (b) histogram of volcanic ash effective radii distribution on April 15, 2010 at 08:00 UTC. 90% of total mass from effective radii of 5–8 μm.

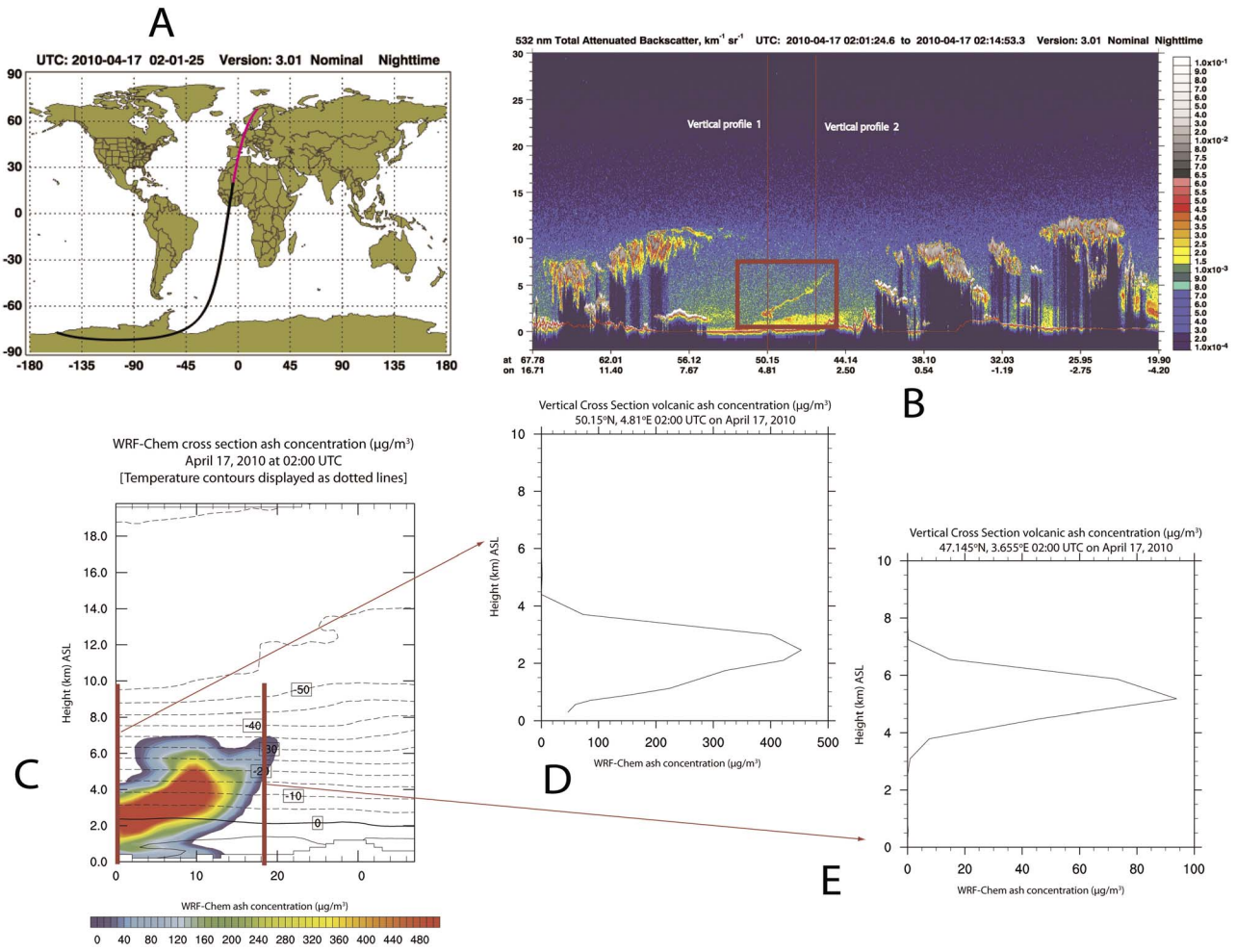

Figure 11. (a) Cloud-Aerosol Lidar and Infrared Pathfinder Satellite Observations (CALIPSO) track, (b) Cloud-Aerosol Lidar and Infrared Pathfinder Satellite Observations (CALIPSO) total attenuated backscatter at 532 nm, (c) Weather Research Forecast coupled with Chemistry (WRF-Chem) modeled vertical slice through model domain as two dimensional slice and vertical profiles (d) 1 and (e) 2 as noted in Figure 11b.

decrease in total mass from April 16–17, relates to a drop in BTD signal as the ash concentration was undetectable by the BTD method. These changes in the total ash mass are not always directly related to changes in total mass, but caveats in the BTD method include changing background surfaces, atmospheric conditions and is the cloud the highest layer? All of which need to be resolved to assess the actual change in volcanic ash mass.

[32] The total number of pixels used in the VAR, (Figure 9b) increased through April 15–16 as more of the ash cloud was determined to be semi-transparent, and therefore detectable with the reverse absorption method. As the ash signal dropped to below the detection limits, the number of pixels in the VAR also diminished. The mean optical depth varied from 0.8 to 0.4 from April 15–16 (Figure 9c). The mean effective radii varied between 5–6 μm throughout the time series (Figure 9d). Within each SEVIRI satellite image, there were a range of measured effective radii (Figure 10) represented by the mean effective radii per image in Figure 9d. Here, with respect to time, the effective radii's of 6–7 μm dominated the distribution (Figure 10a). Significant contributions were provided by effective radii from 4–5, 5–6 and 7–8 μm, see histogram of the individual distributions at 08:00 UTC on April 15 (Figure 10b). Around 80–90% of the total cloud has effective radii between 5–8 μm. The contributions to the total cloud from the super fine effective radii, less than 5 μm, are minimal.

5. Model Comparisons to CALIPSO Data

[33] Additional spaceborne data was available from the NASA/CNES Cloud-Aerosol Lidar and Infrared Pathfinder Satellite Observations (CALIPSO) satellite. CALIPSO comprises three instruments, with the analysis shown here using data from the Cloud-Aerosol Lidar with Orthogonal Polarization (CALIOP) sensor providing nadir-looking full atmospheric column views. On April 17, around 02:00 UTC a CALIPSO (Figure 11a) overpass showed evidence of a backscatter signal from nonmeteorological particles (Figure 11b). This was interpreted as volcanic particles as it passed over Central Western Europe [*Winker et al.*, 2012]. Here the cloud was detected at around 5 km ASL at location

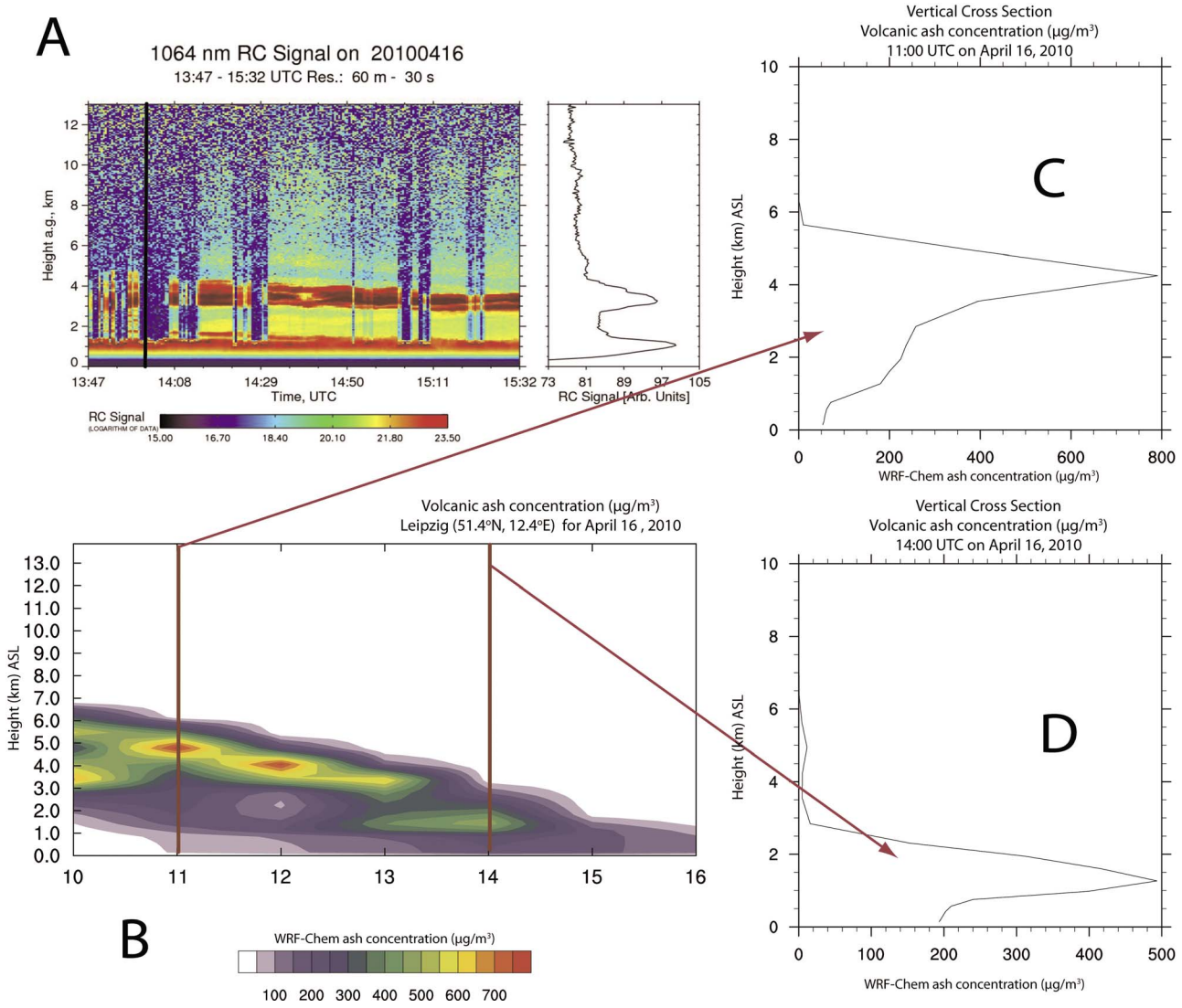

Figure 12. (a) European Aerosol Research Light Detection And Ranging (LIDAR) Network (EARLINET) LIDAR data at Leipzig, Germany on April 16 from 13:47–15:32 UTC, (b) Weather Research Forecast coupled with Chemistry (WRF-Chem) model simulation from 10:00–16:00 UTC and vertical profiles at (c) 11:00 and (d) 14:00 UTC.

44.14°N, 2.50°E and then much lower at around 1–2 km ASL at 50.15°N, 4.81°E (Figure 11b). This relates to an ash cloud at around 5 km ASL sloping toward the surface as it passes from the northwest-southeast direction.

[34] A vertical slice through the WRF-Chem simulation at 02:00 UTC (Figure 11c) provides a comparison to the CALIPSO data, where the higher portion of the modeled cloud is further to southwest (right hand side of cross section in Figure 11b and Figure 11c) at around 4–6 km ASL and lower concentrations also around 1–3 km ASL. A vertical profile at 50.15°N, 4.81°E (Figure 14d located as vertical profile 1 in Figure 11b) showed the modeled cloud in WRF-Chem was low in altitude with the highest modeled concentrations at 2–3 km ASL. The vertical profile at 47.145°N, 3.655°E from WRF-Chem (Figure 11e; located as vertical profile in Figure 11b) showed the highest modeled concentrations at 5–6 km ASL with concentrations dispersed across a region from 3 and 7 km ASL. Altitudes and vertical structure of the modeled ash concentrations from WRF-Chem match well to the CALIOP results showing that the model was able to simulate this detected portion of the cloud in the LIDAR data. Further analysis of the CALIOP would be required to compare absolute concentrations from the two data sets, which is outside the scope of this manuscript.

6. Model Comparison to Ground Observations

[35] As well as satellite based LIDAR data from CALIPSO, the volcanic ash cloud was detected across a number of LIDAR stations in Europe, providing ground observations to compare with WRF-Chem simulations. European Aerosol Research LIDAR Network (EARLINET) stations at Leipzig and Munich, Germany and Paris, France were used. For Leipzig, the LIDAR showed that an ash layer around 3–4 km ASL passed over the region at 13:47–15:32 UTC on April 16, 2010 (Figure 12a). From WRF-

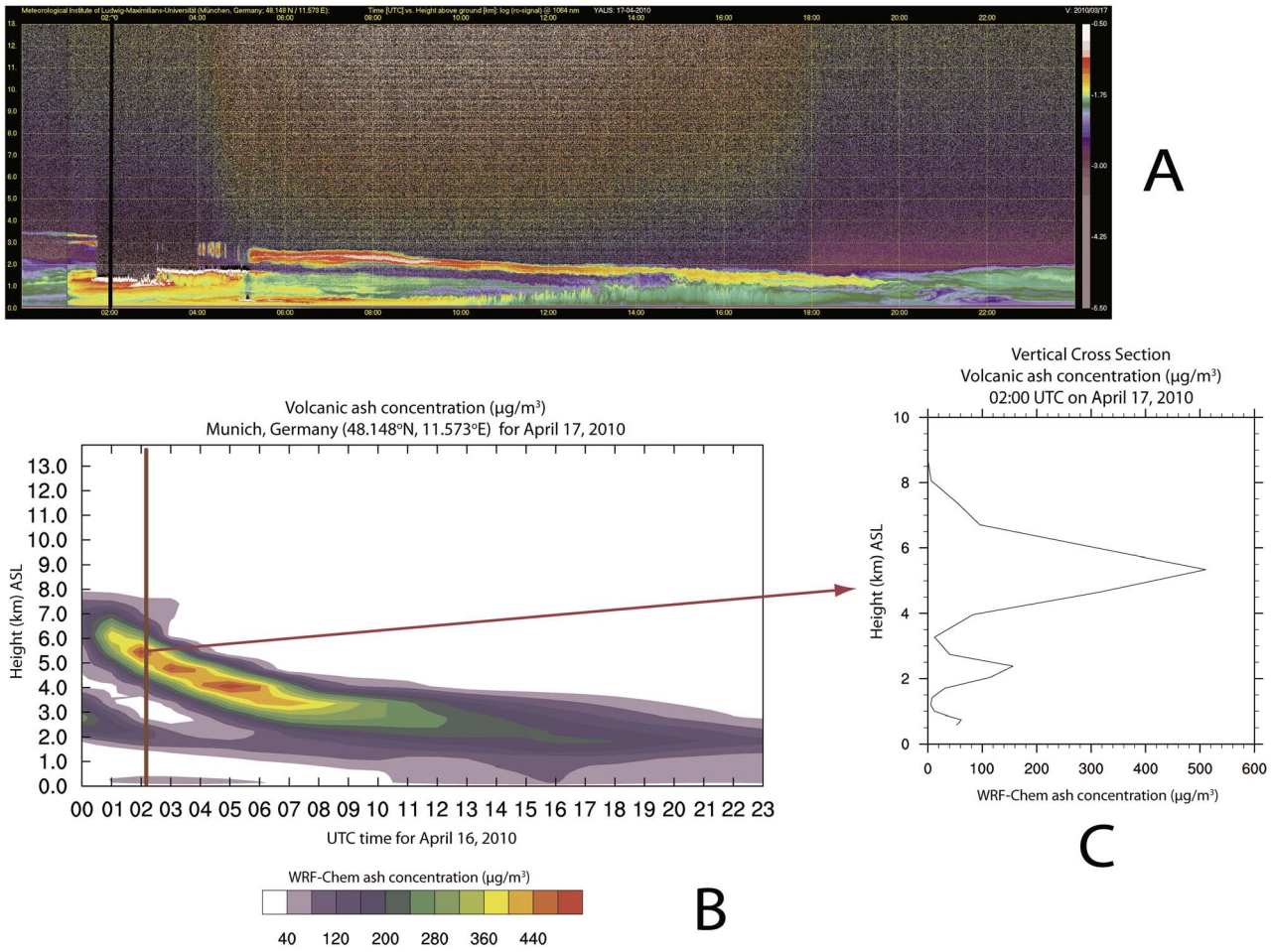

Figure 13. (a) Ceilometer: time-height cross sections from University of Munich LIDAR data at Munich, Germany; (b) Weather Research Forecast coupled with Chemistry (WRF-Chem) model simulation on April 17 from 00:00–23:00 UTC and (c) vertical profile at 02:00 UTC. (see following link for LIDAR Quick look: http://www.meteo.physik.uni-muenchen.de/dokuwiki/doku.php?id=lsmayer:lidar:quicklooks_yalis&pass=1&year_sel=10&mon_sel=04&dsel=17&deriv=.)

Chem, an ash cloud was modeled to pass over between 10:00 and 16:00 UTC. The modeled cloud was around 5 km ASL as it first passed over the site and closer to 2 km ASL by the end (Figure 12b). Modeled ash concentrations at around 11:00 UTC reached 800 μg/m^3 (0.8 mg/m^3), Figure 12c, with the higher modeled concentrations confined from 3–5 km ASL. At 14:00 UTC when the LIDAR observations occurred, WRF-Chem showed a lower altitude, 1–2 km ASL, and lower concentration, 450 μg/m^3, modeled cloud, Figure 12d. *Ansmann et al.* [2010] showed, from post-processed LIDAR data, that the detected ash cloud passed over between 14:15–14:30, was centered around 3.5 km ASL and concentrations around 900 μg/m^3, and as such WRF-Chem simulated concentrations were equivalent in magnitude to the LIDAR data. Noted by *Ansmann et al.* [2010] is the uncertainty estimate of the LIDAR mass concentration (35%) and thus, the modeled mass concentrations are within the uncertainty range of the LIDAR measurements.

[36] Examination of the Munich LIDAR data (Figure 13a; see *Wiegner et al.* [2012] for more details) and the WRF-Chem simulation showed that the model simulated the shape of the ash cloud layer as it passed over the region. Starting 00:00 UTC, the WRF-Chem modeled ash cloud was simulated at 6 km ASL and around 2.5 km ASL by 14:00 UTC. The LIDAR data showed a detectable ash layer at around 3.5 km ASL around 00:00 UTC and at 2 km ASL by 14:00 UTC. The modeled ash concentration levels from WRF-Chem are lower than for the Leipzig location, being closer to 500 μg/m^3. For the same location as the LIDAR data from *Wiegner et al.* [2012], *Ansmann et al.* [2010] retrieved a maximum concentration of 1000 μg/m^3 from post-processed ground based LIDAR profiles, further refined by *Ansmann et al.* [2011] to 1200 μg/m^3 with +−40% error in absolute ash concentration retrieval from ground observations.

[37] The Paris site LIDAR data (Figure 14a) showed an ash layer starting around 16:00 UTC at 6 km ASL and by 23:00 UTC was closer to 4 km ASL, with lower concentrations closer to the ground surface. WRF-Chem showed a modeled ash layer started to pass overhead at 14:00 UTC on April 16 and the highest modeled concentrations passed over closer to 02:00–04:00 UTC on April 17. The WRF-Chem simulation showed this higher modeled concentrations (Figure 14b) started at 6 km ASL and with time ash at lower

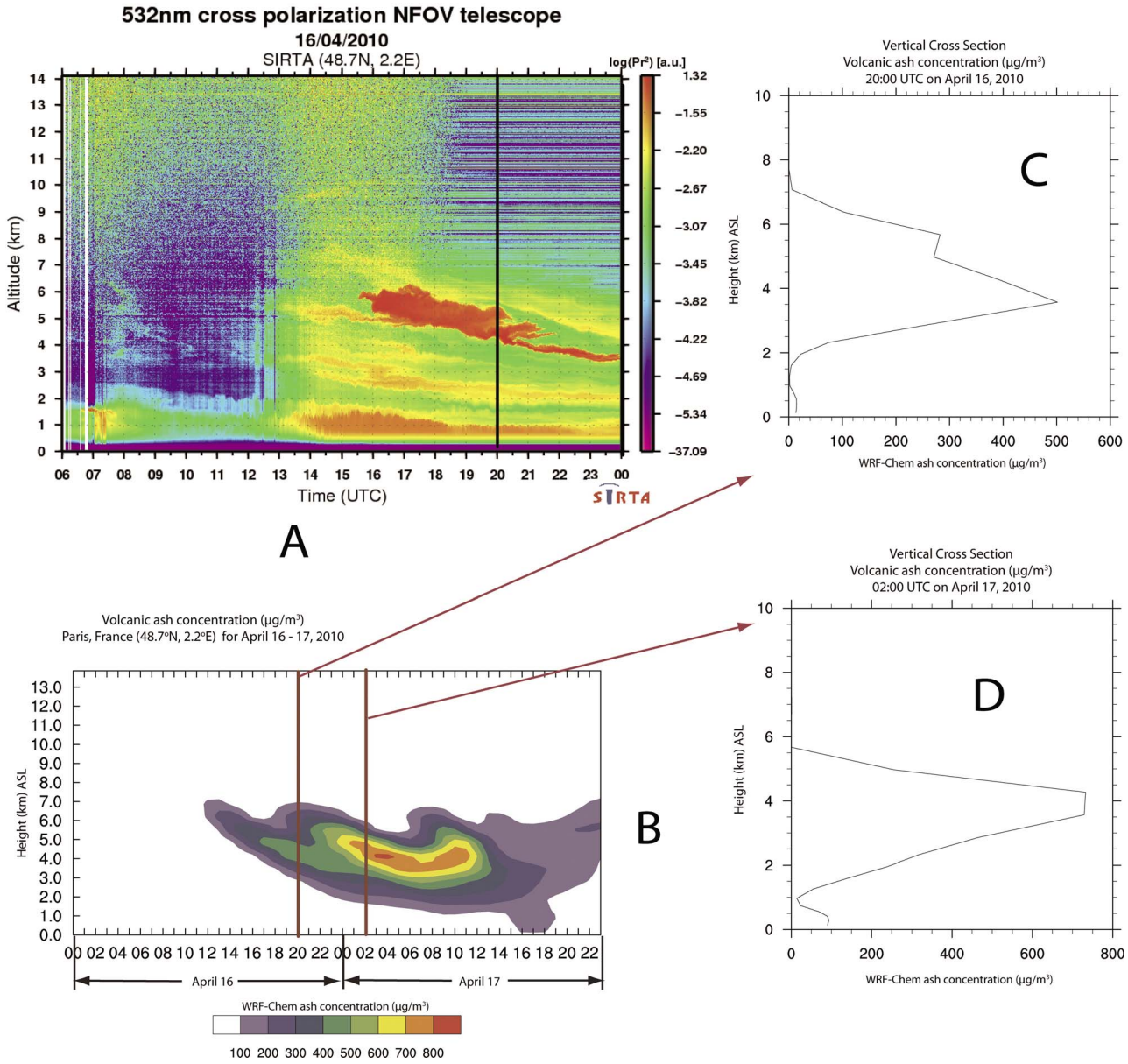

Figure 14. (a) European Aerosol Research Light Detection And Ranging (LIDAR) Network (EARLINET) LIDAR data at Paris, France from 06:00 April 16–00:00 UTC April 17; (b) Weather Research Forecast coupled with Chemistry (WRF-Chem) model simulation on April 16/17 from 00:00–23:00 UTC and vertical profiles at (c) 20:00 UTC on April 16 and (d) 02:00 UTC on April 17, 2010.

altitudes passed over Paris. This cloud shape broadly matches that seen in the LIDAR data, if a 6 h later. Concentrations from WRF-Chem at 20:00 UTC on April 16 and 02:00 UTC on April 17 were around 800 μg/m^3 (Figure 14c and Figure 14d) with the layer centered around 4–6 km ASL. The LIDAR data and modeled ash cloud matched well in terms of the vertical structure. No direct comparisons could be made to the absolute concentrations. For the WRF-Chem modeling, note that the downwind concentrations are heavily dependent on the initial imputed mass eruption rate, timing and total mass in the fine ash bins.

[38] Additional, post processed LIDAR data from *Emeis et al.* [2011] and *Gasteiger et al.* [2011] has also shown that the WRF-Chem simulations match well in space and time with the ground observations across Southern Germany, though the concentrations were slightly lower in the modeling results. *Gasteiger et al.* [2011] showed concentrations between 650–1800 μg/m^3 across Southern Germany; whereas the WRF-Chem simulation concentrations are closer to 450–550 μg/m^3. The WRF-Chem model results were at the lower end of the observed concentrations, but again with up to 35% variability with the post-processed LIDAR measurements [*Ansmann et al.*, 2010], the modeled results are within the LIDAR uncertainty limits.

[39] To be able to convert satellite remote sensing retrievals of mass loadings an assumption is often made a 1 km thick ash

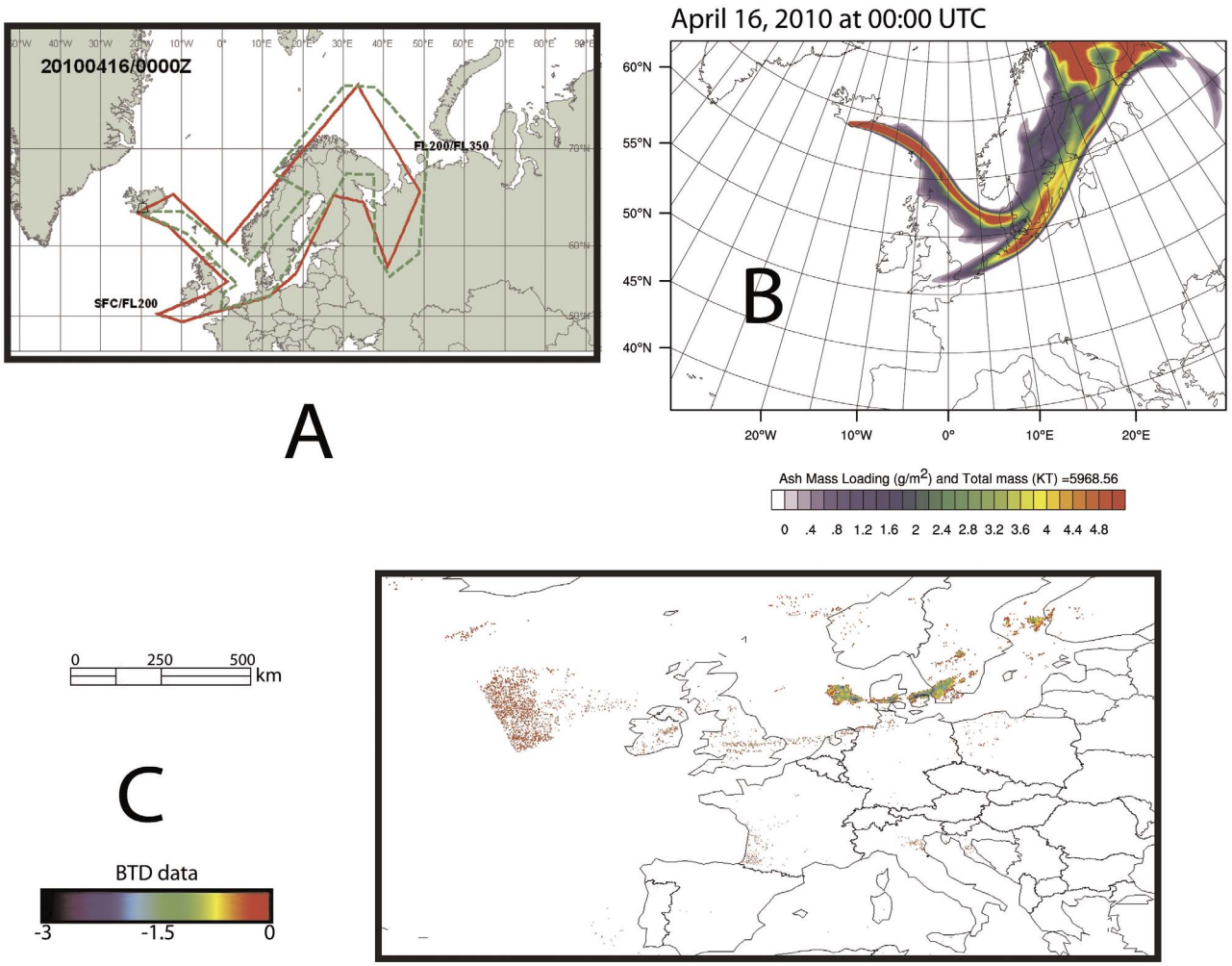

Figure 15. (a) London Volcanic Ash Advisory Center (VAAC) boundaries, (b) Weather Research Forecast coupled with Chemistry (WRF-Chem) modeled integrated ash mass loading and (c) brightness temperature difference (BTD) map from −3 to 0 K for April 16, 2010 at 00:00 UTC.

cloud to be able to convert the mass loadings in g/m^2 into g/m^3 for an airborne ash concentration. This might not be true for all ash clouds. For modeling of ash clouds, the initial vertical structure and particle size distribution will affect the downwind modeled cloud thickness. The modeled data for Paris, Leipzig and Munich showed that the WRF-Chem modeled cloud was not defined over a 1 km region but was broadly defined within the lower levels of the atmosphere. Satellite remote sensing is able to determine the total mass (kt) in the atmosphere. For Leipzig, Figure 12, at 11:00 UTC on April 16, 2010 WRF-Chem showed a total mass of 552 T within the 324 km^2 WRF-Chem grid cell for the defined vertical structure seen in Figure 12c. If assuming this modeled cloud to be 1 km thick, a maximum concentration would be 1700 mg/m^3, for assuming the cloud to be 3 km thick, the maximum concentration would be 570 mg/m^3 and for assumed 8 km thick cloud, the maximum concentration would be 210 mg/m^3. Here, to compare the modeled ash cloud to the satellite data requires a direct analysis of the mass loading within the full column, removing the assumptions of a 1 km thick cloud. Results of this comparison can then be used to ascertain the level of reliability in the three-dimensional ash concentrations from the modeled cloud.

7. Discussion of WRF-Chem Results

[40] The analysis here has compared the adaptation of the WRF-Chem model for volcanic ash modeling to (1) satellite retrieved ash clouds from SEVIRI data; (2) satellite based CALIPSO LIDAR and (3) several ground based LIDAR data. For VATD models to produce accurate volcanic ash concentrations predictions, input parameters like total grain size distribution, total erupted mass, initial plume height, event duration and vertical distribution need to be known as accurate as possible. The downwind concentrations will be most sensitive to either the plume height to mass flux calculations or the weighting of the total mass within the volcanic ash particle bins. Figure 15 shows a snapshot from April 16, 2010 at 00:00 UTC comparing the VAAC produced volcanic ash advisory graphic (VAG) during the eruptive events, the WRF-Chem modeled ash cloud, and the SEVIRI data. Here, there is good agreement between all. The satellite detects an ash cloud over a smaller region, as a

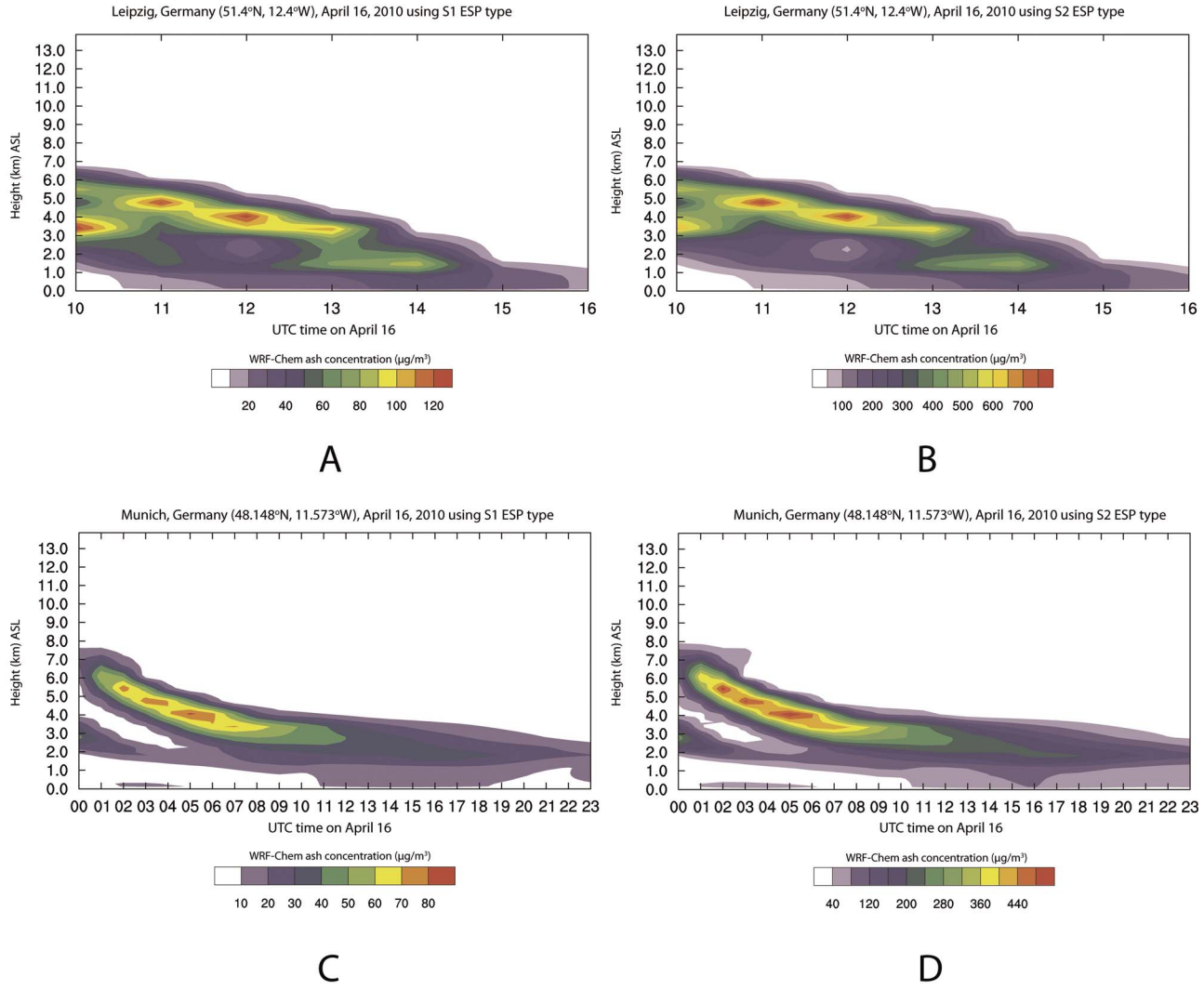

Figure 16. Comparisons of time slices through Weather Research Forecast coupled with Chemistry (WRF-Chem) model simulations with two different particle size distributions, eruption source parameter (ESP) type S1 and S2 respectively. (a and b) Lidar site at Leipzig, Germany from 10:00–16:00 UTC on April 16. (c and d) Lidar site at Munich, Germany from 00:00–23:00 UTC on April 16, 2010.

result of both local meteorological clouds and the ash concentrations below the detection limits of the sensor and retrieval method.

[41] In volcanic ash transport and dispersion, the NWP spatial and temporal domains are important parameters in the model simulations. Most VATD models will use a predefined and pre-generated NWP data set for its advection. WRF-Chem, with its volcanic ash transport and numerical weather prediction data generated on the same spatial and temporal domain, allows volcanic ash simulations to be performed for any time period and any location, with the user control on the NWP data. The VATD model simulation is not limited by the NWP spatial domain or time scales for the forecast. As such, the WRF-Chem model can provide three-dimensional fields of atmospheric temperature, pressure and water vapor along with the modeled ash concentrations. This information is an essential tool where comparing the satellite to model data, as water vapor and ice content in the cloud can be limiting factors in the use of the reverse absorption method [*Prata et al.*, 2001]. In addition, this NWP data can be used for atmospheric corrections of thermal infrared measurements, such as the approaches of *Yu et al.* [2002] using the moderate resolution transmission (MODTRAN) analysis system as well as the synthetic BTD map approach of *Millington et al.* [2012].

[42] For the analyses shown in this manuscript for Eyjafjallajökull, the ESP S2 type particle size distribution was assigned to the eruptive events. *Mastin et al.* [2009] provide 10 different eruption types. To compare the significance of the initial size distribution on the downwind concentrations, the ash cloud from Eyjafjallajökull was modeled using the S1 particle size distribution in comparison to the S2 type to test the sensitivity on the downwind ash concentrations. The S1 type has 10% of the total eruptive mass for particles less than 63 μm in diameter, whereas S2 has 40% of the mass for these particle ranges. For the two simulations, the same empirical relationship for the eruption rate as well as the same umbrella shape vertical distribution were used. The

two LIDAR sites at Leipzig and Munich were chosen to compare the simulation results, Figure 16. Both sites showed a good agreement in the shape and timing of the clouds using the S1 or S2 type.

[43] The greatest difference was in the magnitude of the ash concentrations. Leipzig site showed concentrations for S1 type with a maximum of 140 $\mu g/m^3$ and for S2 a maximum of 800 $\mu g/m^3$, Figure 16a and Figure 16b respectively. For Munich, the differences are 90 to 520 $\mu g/m^3$, Figure 16c and Figure 16d respectively. The S2 type concentrations are of similar magnitude to the LIDAR measurements. During an operational setting, the real particle size distribution is unknown. For this Eyjafjallajökull case with a umbrella vertical distribution and using the empirical relationship between eruption rate and plume height, the ESP S2 type gave good results to the measured ground observations, with modeled ash concentrations within the error limits of the post-processed LIDAR observations. Knowing if the assigned ESP type is correct is critical to forecast ash concentrations to the level of accuracy of 1–4 mg/m^3. Note that the initial vertical distribution and methodology for initial eruption rate calculation are also critical model input parameters.

[44] WRF-Chem like other VATD models [*WMO*, 2010] does not take account of aggregation processes. Most models will load the mass fraction into the coarser ash bins to account for aggregation. If finer particles were to aggregate, then they would settle out quicker, as they obtain a greater mass and settling rate in their aggregate form. Recent work for Eyjafjallajökull has shown that improved matches between models and observations occur when 10% of mass is within the fine ash bins [*Dacre et al.*, 2011]. This shows that perhaps, we have 40% of ash mass in fine bins at the onset but 30% of this is removed through aggregation. Running VATD models with 10% of the initial erupted mass as fine ash will 'account' for aggregation. So, The VATD simulation will transport the fine ash downwind and then the modeled clouds will have a closer match to the satellite and ground observations. This approach first assumes that the eruption rate and hence total erupted mass is accurate as well as providing an inaccurate coarser ash fraction and hence inaccurate ashfall. A better approach would be to account for particle-to-particle aggregation within the VATD but more work is required to allow dynamic volcanic ash models to account for aggregations without having to solve directly. i.e., some form of model parameterization.

[45] In addition to the initial particle size distribution, the accuracy of the eruption rate used in the modeling of the ash cloud is critical. Using the *Mastin et al.* [2009] empirical relationship, we applied the rate of erupted ash using the measured plume height. *Mastin et al.* [2009] state a factor of 50% probability of being within a factor of 4 from the empirical relationship. Therefore, for a 5 km ASL cloud, there is a 50% probability of the eruption rate varying from $5.6*10^4$ kg/s to $2.2*10^5$ kg/s. We applied a mean of $1.1*10^5$ kg/s, i.e., direct conversion from measured plume height using the empirical equations from *Mastin et al.* [2009]. Such differences in eruption rate need to be compared to actual eruption rates as they can significantly affect any comparisons of the downwind mass loadings from the modeled cloud to the measured ash signal. Coupled with knowing the correct particle size distribution, the mass loadings can vary by factors greater than 10. The total mass to be included in the WRF-Chem simulation could also vary considerably based on the accuracy in the plume height measurement. As the *Mastin et al.* [2009] relationship compared the plume height to the eruption rate, then as the measured plume height increases, the sensitivity of the mass fluxes to the accuracy of the plume height lessons. Most volcanic eruptions will be detected from satellite remote sensing, and generally in timely manner from infrared data, and hence could have associated inaccuracies in their conversion from measured cloud top temperature to plume height measurements. For these Eyjafjallajökull events, the empirical relationships showed for a 5.5 km ASL plume, that an inaccuracy of 0.25 km (measured to be 5.5 km but could be either 5.25 or 5.75 km ASL) would change the calculated mass flux by up to 30%.

[46] The WRF-Chem simulation showed volcanic ash concentrations around 500–1000 $\mu g/m^3$ (0.5–1.0 mg/m^3) as the cloud passed across mainland Europe. As it reached mainland Europe, the ash cloud was sheared in a southwest-northeast direction and as such the concentrations dropped to close to 1000 $\mu g/m^3$ (1.0 mg/m^3). At several LIDAR stations, WRF-Chem showed good agreement in space and time, with similar orders of magnitude when compared to the post-processed LIDAR concentrations. In southern Germany, concentrations from WRF-Chem were around 300–400 $\mu g/m^3$ (0.3–0.4 mg/m^3) compared to the LIDAR data of 650–1800 $\mu g/m^3$ (0.65–1.8 mg/m^3). The WRF-Chem simulations used around 19% of the eruptive mass in bins 7 and 8 (7.81–31.25 μm particles in diameter). *Stohl et al.* [2011] found with inverse modeling of the satellite data that around 10% of the total mass was from particles between bins 7 and 8, compared to 40% in WRF-Chem. They showed a good agreement to the satellite data and used the Plumeria model [*Mastin*, 2007] to determine the eruption rate. Satellite data results would be for detected ash particles from 0–50 μm in radii. Infrared retrievals provide an effective radii, measured from the thermal infrared at-sensor radiance difference at two TIR wavelengths and an assumed lognormal distribution. For comparison to WRF-Chem concentrations, this would be for particles 0–100 μm in diameter.

[47] So why might the two approaches be different? Eruption rate is a critical component here along with the local wind conditions [*Bursik et al.*, 2009]. For example a recorded 9 km ASL plume which was bent over from cross winds would be much higher eruption rate than for an eruption column recorded at the same altitude but unaffected by winds. *Bursik* [2001] showed that for a 20 km ASL plume and no cross plume wind, then the eruption rate is 2×10^6 kg/s compared the case with a mean cross wind of 25 m/s (90 km/h), where eruption rate would need to be 2×10^8 kg/s, an increase of 100 fold. So if we reduce the fine ash to 10% of the total mass and increase the eruption rate by 4 times than from *Mastin et al.* [2009] method, you would have the same total mass and thus a good match to the LIDAR measurements and satellite retrievals. Further work is required to determine how a cross wind would affect the eruption rate for this April period of the Eyjafjallajökull eruption. Additionally, *Kaminski et al.* [2011] approached the partitioning of the erupted mass between the ground flow and plume and stated that the classic model for a Plinian model would have overestimated mass eruption rate by up to 20%. Again, their

analysis shows that classical plume theory or empirical relationships from measured plume heights can generate significant variations in the eruption rate and hence downwind distal ash concentrations.

[48] Definition of the initial plume shape can be a critical component to fully represent the true ash plume shape. WRF-Chem has the plume defined by a umbrella shaped or Gaussian vertical distribution (Stuefer et al., submitted manuscript, 2012). However, did the Eyjafjallajökull eruption plume have a true umbrella shaped vertical distribution? *Dacre et al.* [2011] emitted the volcanic ash uniformly in the vertical for their NAME analysis. The PUFF VATD model has options for a uniform or exponential shape in the vertical [*Peterson*, 2006]. Further work is required to assess the effect of initial plume vertical distribution on downwind modeled ash cloud movement and mass loadings. *Bursik* [2001] provides an approach to determine plume vertical structure based on local atmospheric conditions and volcanological parameters like eruption rate, release velocity, vent diameters and latent heat release. Adaption of the Stuefer et al. (submitted reference, 2012) plume model for WRF-Chem with the PUFF VATD options and *Bursik* [2001] approach would provide an improvement to the WRF-Chem for the multiple potential eruption plumes that can occur from a volcanic event.

[49] The model simulations showed that an ash layer around 5 km ASL passed across Continental Europe through April 15–18, 2010, with variable concentrations at different levels. The modeled ash cloud was not a simple one layer passing overhead. Ash was seen from the surface to 6 km ASL from both satellite and ground based sensors. WRF-Chem was able to capture the ash layers seen in these measurements. The SEVIRI volcanic ash retrievals showed an ash cloud passing across mainland Europe (Figures 7 and 8) but no evidence of any ash across the United Kingdom. The BTD data (Figure 8) showed a positive signal traveling parallel to the negative portion of the cloud. This could be either volcanic ash coated in ice, *Rose et al.* [2003] state this can reverse the BTD signal, or meteorological cloud associated to the eruption cloud. This portion would have been advected westerly toward to the UK. *Devenish et al.* [2012] and *Dacre et al.* [2011] showed that mass loadings of 0.37 g/m^2 were detected at several LIDAR sites in the UK.

[50] WRF-Chem model simulations have shown that they can help to determine not only the absolute concentration but also the altitude range where a threshold may be breached that is critical to the aviation community. Column averaged ash concentrations might not exceed these limits, but may at certain elevations. Averaging concentrations over defined vertical levels could mask out these higher concentrations peaks. When comparing to satellite data retrievals of the volcanic ash clouds, mass loadings are required from both the satellite data and modeled ash cloud. This removes the assumption required to convert the satellite data from mass loading to column averaged concentrations. Additionally, approaches, like those of *Millington et al.* [2012] where modeled ash cloud is used to simulate the volcanic ash imagery and then BTD maps are calibrated and validated, could be applied to operational setting. For comparison to ground observations, the full three-dimensional ash column is required to calibrate and validate the model simulations.

[51] To assist in hazard mitigation, the next step is to determine the mass loading levels that the TIR sensors can detect volcanic ash, and whether satellites can detect an ash cloud below this threshold. This is currently being discussed within the International Volcanic Ash Task Force and Volcanic Ash Scientific Advisory Group [*IVATF*, 2011]. With accurate input parameters, volcanic ash dispersion and transport models can provide this limiting threshold and assist in the awareness of potentially hazards ash concentrations to the aviation community.

8. Conclusions

[52] In April and May 2010, Eyjafjallajökull, Iceland had a large explosive volcanic eruption, with ash reaching up to 9 km above sea level and being advected toward mainland Europe [*Gudmundsson et al.*, 2010]. Here, we have focused on the first few days of the explosive period from April 14–19, 2010 using a newly developed adaption of the Weather Research and Forecasting (WRF)-Chemistry (WRF-Chem) model for volcanic ash clouds. The dispersing ash from the April events was detected on SEVIRI satellite remote sensing data using the brightness temperature difference data and reverse absorption methods. The WRF-Chem model was able to simulate the ash plumes and dispersing clouds during the 5 day period. Initial model inputs, such as eruption rate and grain size distribution were derived from the eruption source parameters of *Mastin et al.* [2009]. Other information on plume altitude and duration were available from the IMO (online data, 2010).

[53] Our work has shown that the fine particles (15.6 μm or less in diameter) modeled from WRF-Chem were those detected and observed in the LIDAR data and over the rest of Europe. Therefore, the initial distribution in the model requires the percentage of the total volcanic mass in these particle size bins to be known with the most accuracy for the WRF-Chem and LIDAR data to match. Variations in the eruption rate from the empirical relationship if the real atmospheric conditions are taken into account are needed to be analyzed with the fine ash fraction. As seen in our WRF-Chem simulations, ash particles greater than 125 μm in diameter will fallout of the atmospheric under gravitational settling. The weighting of the total mass in each particle size bin is generally unknown during an eruption and a particle size distribution is required to produce airborne concentrations. The ESP data sets are therefore the best tool available for an operational event, until more is known about the initial grain size distribution.

[54] Analysis by *Dacre et al.* [2011] showed that downwind concentrations from the modeling of the Eyjafjallajökull eruption cloud had the best agreement to the ground observations with the fine ash fraction of the eruptive mass at 10%. Our analysis showed the best agreement to be closer for 40% of the eruptive mass, with the *Mastin et al.* [2009] empirical eruption rate approach. However, the eruption rate is a significant parameter here as changes in the eruption rate, using the empirical approach, have a 50% probability of varying by a factor of 4 (within errors of *Mastin et al.* [2009] empirical relationship). Therefore, the fine ash fraction could also vary by a factor of 4 given the particular choice of eruption rate. Additionally, the aggregation effect, not accounted for in WRF-Chem or the *Dacre et al.* [2011]

analysis, could again provide different downwind mass loadings. If one includes the potential variability in the initial plume vertical distribution into the mix and a large number of VATD model inputs exists where their variability can cause downwind modeled mass loadings to vary by factors greater than 10.

[55] In summary, our analysis has shown that the measured plume height, eruption rate, timing and particle size distributions are all critical components for producing useful downwind ash concentrations to the levels of 0.5–1 mg/m^3. The measured plume height and its level of accuracy will be critical in determining the mass flux rate and total erupted mass. The timing and knowledge of when there are changes in initial plume height are critical to accurate forecast where ash cloud will disperse. The percentages of total mass within each defined particle bins will determine the amount of volcanic ash that can be advected downwind. Volcanic ash will be advected by the local weather patterns, but one needs to know how much fine ash is in the eruption cloud for the model simulations.

[56] The fusion of data from volcanic ash transport and dispersion models, such as WRF-Chem, with satellite thermal infrared remote sensing data, seen here from SEVIRI, and other satellite and ground based observations, as shown here with LIDAR, is the way forward for those performing volcanic ash cloud mitigation. As satellite remote sensing data becomes available and ground observations record the location of an ash cloud, this data needs to be included within the model forecasts to constrain the modeled mass loadings. Further model forecasts from these new ash cloud mass loadings will provide a forecast closer to the observations. Continuing this iteration as more data is available is needed within volcanic ash cloud modeling. Obtaining as much information about the ash cloud is critical to produce the best hazard assessment and provide risk mitigation strategies for the aviation industry and human populations.

[57] **Acknowledgments.** We thank the University of Wisconsin for archived SEVIRI data, Barbara Stunder at Air Resource Laboratories, NOAA, for the HYSPLIT model data and the American Recovery and Reinvestment Act (ARRA) grant. Additionally, we thank the Arctic Region Supercomputing Center, UAF, for their assistance in providing computing time for the WRF-Chem model simulations. This publication is the results in part of research sponsored by the Cooperative Institute for Alaska Research with funds from the National Oceanic and Atmospheric Administration under cooperative agreement NA08OAR4320751 with the University of Alaska. We would like to thank the three anonymous reviewers of the manuscript, who provided useful and detailed comments on the analysis performed and allowed us to construct an improved manuscript. The views, opinions, and findings contained in this report are those of the authors and should not be construed as an official National Oceanic and Atmospheric Administration or U.S. Government position, policy, or decision.

References

Ansmann, A., et al. (2010), The 16 April 2010 major volcanic ash plume over central Europe: EARLINET lidar and AERONET photometer observations at Leipzig and Munich, Germany, *Geophys. Res. Lett.*, *37*, L13810, doi:10.1029/2010GL043809.

Ansmann, A., et al. (2011), Ash and fine-mode particle mass profiles from EARLINET-AERONET observations over central Europe after the eruptions of the Eyjafjallajökull volcano in 2010, *J. Geophys. Res.*, *116*, D00U02, doi:10.1029/2010JD015567.

Bailey, J. E., K. G. Dean, J. Dehn, and P. W. Webley (2010), Integrated satellite observations of the 2006 eruption of Augustine Volcano, *U.S. Geol. Surv. Prof. Pap.*, *1769*, 481–506.

Bursik, M. (2001), Effect of wind on the rise height of volcanic plumes, *Geophys. Res. Lett.*, *28*(18), 3621–3624, doi:10.1029/2001GL013393.

Bursik, M. I., S. E. Kobs, A. Burns, O. A. Braitseva, L. I. Bazanova, I. V. Melekestsev, A. Kurbatov, and D. C. Pieri (2009), Volcanic plumes and wind: Jet stream interaction examples and implications for air traffic, *J. Volcanol. Geotherm. Res.*, *186*(1–2), 60–67.

Carey, S. (1986), Modeling of tephra fallout from atmospheric eruptions, in *Monitoring and Mitigation of Volcanic Hazards*, edited by L. A. Scarpa and R. I. Tilling, pp. 429–463, Springer, Berlin.

Casadevall, T. J. (1994), The 1989–1990 eruption of Redoubt Volcano Alaska: Impacts on aircraft operations, *J. Volcanol. Geotherm. Res.*, *62*(1–4), 301–316, doi:10.1016/0377-0273(94)90038-8.

Chazette, P., M. Bocquet, P. Royer, V. Winiarek, J.-C. Raut, P. Labazuy, M. Gouhier, M. Lardier, and J.-P. Cariou (2012), Eyjafjallajökull ash concentrations derived from both lidar and modeling, *J. Geophys. Res.*, *117*, D00U14, doi:10.1029/2011JD015755.

Dacre, H. F., et al. (2011), Evaluating the structure and magnitude of the ash plume during the initial phase of the 2010 Eyjafjallajökull eruption using lidar observations and NAME simulations, *J. Geophys. Res.*, *116*, D00U03, doi:10.1029/2011JD015608.

D'Amours, R., and A. Malo (2004), A zeroth order Lagrangian particle dispersion model: MLDP0, internal document, 18 pp., Environ. Emergency Response Sect., Can. Meteorol. Cent., Dorval, Que., Canada.

Dean, K. G., J. Dehn, K. P. Papp, S. Smith, P. Izbekov, R. Peterson, C. Kearney, and A. Steffke (2004), Integrated satellite observations of the 2001 eruption of Mt. Cleveland, Alaska, *J. Volcanol. Geotherm. Res.*, *135*, 51–73, doi:10.1016/j.jvolgeores.2003.12.013.

Devenish, B. J., D. J. Thomson, F. Marenco, S. J. Leadbetter, H. Ricketts, and H. F. Dacre (2012), A study of the arrival over the United Kingdom in April 2010 of the Eyjafjallajökull ash cloud using ground-based lidar and numerical simulations, *Atmos. Environ.*, *48*, 152–164, doi:10.1016/j.atmosenv.2011.06.033.

Draxler, R. R., and G. D. Hess (1998), An overview of the Hysplit_4 modeling system for trajectories, dispersion, and deposition, *Aust. Meteorol. Mag.*, *47*, 295–308.

Durant, A. J., and W. I. Rose (2009), Sedimentological constraints on hydrometeor-enhanced particle deposition: 1992 eruptions of Crater Peak, Alaska, *J. Volcanol. Geotherm. Res.*, *186*, 40–59, doi:10.1016/j.jvolgeores.2009.02.004.

Emeis, S., et al. (2011), Measurement and simulation of the 16/17 April 2010 Eyjafjallajökull volcanic ash layer dispersion in the northern Alpine region, *Atmos. Chem. Phys.*, *11*, 2689–2701, doi:10.5194/acp-11-2689-2011.

European Space Agency (2011), Definition of SEVIRI channels and characteristics of MSG Images. Annex III, report, Paris. [Available at http://eopi.esa.int/doc/msg/description/data/msg-rao-annex3.pdf.]

Francis, P. N., M. C. Cooke, and R. W. Saunders (2012), Retrieval of physical properties of volcanic ash using Meteosat: A case study from the 2010 Eyjafjallajökull eruption, *J. Geophys. Res.*, *117*, D00U09, doi:10.1029/2011JD016788.

Freitas, S. R., K. M. Longo, M. F. Alonso, M. Pirre, V. Marecal, G. Grell, R. Stockler, R. F. Mello, and M. Sánchez Gácita (2011), PREP-CHEM-SRC 1.0: A preprocessor of trace gas and aerosol emission fields for regional and global atmospheric chemistry models, *Geosci. Model Dev.*, *4*, 419–433, doi:10.5194/gmd-4-419-2011.

Gasteiger, J., S. Groß, V. Freudenthaler, and M. Wiegner (2011), Volcanic ash from Iceland over Munich: Mass concentration retrieved from ground-based remote sensing measurements, *Atmos. Chem. Phys.*, *11*, 2209–2223, doi:10.5194/acp-11-2209-2011.

Grell, G. A., and A. Baklanov (2011), Integrated modeling for forecasting weather and air quality: A call for fully coupled approaches, *Atmos. Environ.*, *45*, 6845–6851, doi:10.1016/j.atmosenv.2011.01.017.

Grell, G., S. E. Peckham, R. Schmitz, S. A. McKeen, G. Frost, W. C. Skamarock, and B. Eder (2005), Fully coupled "online" chemistry within the WRF model, *Atmos. Environ.*, *39*, 6957–6975, doi:10.1016/j.atmosenv.2005.04.027.

Gudmundsson, M. T., R. Pedersen, K. Vogfjörd, B. Thorbjarnardóttir, S. Jakobsdóttir, and M. J. Roberts (2010), Eruptions of Eyjafjallajökull Volcano, Iceland, *Eos Trans. AGU*, *91*(21), 190–191, doi:10.1029/2010EO210002.

Hansen, J. E., and L. D. Travis (1974), Light-scattering in planetary atmospheres, *Space Sci. Rev.*, *16*, 527–610, doi:10.1007/BF00168069.

International Volcanic Ash Task Force (IVATF) (2011), IVATF Task TF-SCI03 Progress report (Part 1)—Understanding visible ash, paper presented at IVATF/2 Meeting, IVATF, Montreal, Que., Canada. [Available at http://www2.icao.int/en/anb/met/ivatf/Documents/IVATF.2.WP.008.2.en.pdf.]

Jones, A., D. Thomson, M. Hort, and B. Devenish (2007), The U.K. Met Office's Next-Generation Atmospheric Dispersion Model, NAME III, in *Air Pollution Modeling and Its Applications XVII*, pp. 580–589, Springer, New York.

Kaminski, E., S. Tait, F. Ferrucci, M. Martet, B. Hirn, and P. Husson (2011), Estimation of ash injection in the atmosphere by basaltic volcanic plumes: The case of the Eyjafjallajökull 2010 eruption, *J. Geophys. Res.*, *116*, B00C02, doi:10.1029/2011JB008297.

Madonna, F., A. Amodeo, G. D'Amico, L. Mona, and G. Pappalardo (2010), Observation of non-spherical ultragiant aerosol using a microwave radar, *Geophys. Res. Lett.*, *37*, L21814, doi:10.1029/2010GL044999.

Mastin, L. G. (2007), A user-friendly one-dimensional model for wet volcanic plumes, *Geochem. Geophys. Geosyst.*, *8*, Q03014, doi:10.1029/2006GC001455.

Mastin, L. G., et al. (2009), A multidisciplinary effort to assign realistic source parameters to model of volcanic ash-cloud transport and dispersion during eruptions, *J. Volcanol. Geotherm. Res.*, *186*(1–2), 10–21.

Millington, S. C., R. W. Saunders, P. N. Francis, and H. N. Webster (2012), Simulated volcanic ash imagery: A method to compare NAME ash concentration forecasts with SEVIRI imagery for the Eyjafjallajökull eruption in 2010, *J. Geophys. Res.*, *117*, D00U17, doi:10.1029/2011JD016770.

Newhall, C. G., and S. Self (1982), The volcanic explosivity index (VEI): An estimate of explosive magnitude for historical volcanism, *J. Geophys. Res.*, *87*(C2), 1231–1238, doi:10.1029/JC087iC02p01231.

Oberhuber, J. M., M. Herzog, H.-S. Graf, and K. Schwanke (1998), Volcanic plume simulation on large scales, *J. Volcanol. Geotherm. Res.*, *87*(1–4), 29–53, doi:10.1016/S0377-0273(98)00099-7.

Pavolonis, M. J. (2010), Advances in extracting cloud composition information from spaceborne infrared radiances: A robust alternative to brightness temperatures. Part I: Theory, *J. Appl. Meteorol. Climatol.*, *49*, 1992–2012, doi:10.1175/2010JAMC2433.1.

Pavolonis, M., and M. Sieglaff (2010), GOES-R Advanced Baseline Imager (ABI) algorithm theoretical basis document for volcanic ash (detection and height), *NOAA CSTAR Tech. Doc. Ver. 2.0*, 72 pp., NOAA, Camp Springs, Md.

Peterson, R. (2006), Puff volcanic ash transport and dispersion model user manual, report, 44 pp., Univ. of Alaska Fairbanks, Fairbanks. [Available at http://puff.images.alaska.edu/doc/puff_user_manual.pdf.]

Peterson, R., P. W. Webley, R. DAmours, R. Servranckx, R. Stunder, and K. Papp (2012), Volcanic ash cloud dispersion models, in *Volcanoes of the North Pacific: Observations from Space*, Springer, New York, in press.

Prata, A. J. (1989a), Infrared radiative transfer calculations for volcanic ash clouds, *Geophys. Res. Lett.*, *16*, 1293–1296, doi:10.1029/GL016i011p01293.

Prata, A. J. (1989b), Observations of volcanic ash clouds in the 10–12 μm window using AVHRR/2 data, *Int. J. Remote Sens.*, *10*, 751–761, doi:10.1080/01431168908903916.

Prata, A. J., and I. F. Grant (2001), Retrieval of microphysical and morphological properties of volcanic ash plumes from satellite data: Application to Mt. Ruapehu, New Zealand, *Q. J. R. Meteorol. Soc.*, *127*, 2153–2179, doi:10.1002/qj.49712757615.

Prata, A. J., and A. T. Prata (2012), Eyjafjallajökull volcanic ash concentrations determined using Spin Enhanced Visible and Infrared Imager measurements, *J. Geophys. Res.*, *117*, D00U23, doi:10.1029/2011JD016800.

Prata, F., G. Bluth, W. Rose, D. Schneider, and A. Tupper (2001), Comments on "Failures in detecting volcanic ash from a satellite-based technique," *Remote Sens. Environ.*, *78*, 341–346, doi:10.1016/S0034-4257(01)00231-0.

Rose, W. I., G. J. S. Bluth, D. J. Schneider, G. G. J. Ernst, C. M. Riley, L. J. Henderson, and R. G. McGimsey (2001), Observations of volcanic clouds in their first few days of atmospheric residence; the 1992 eruptions of Crater Peak, Mount Spurr Volcano, Alaska, *J. Geol.*, *109*(6), 677–694, doi:10.1086/323189.

Rose, W. I., et al. (2003), The February-March 2000 eruption of Hekla, Iceland from a satellite perspective, in *Volcanism and the Earth's Atmosphere*, *Geophys. Monogr. Ser.*, vol. 139, edited by A. Robock and C. Oppenheimer, pp. 107–132, AGU, Washington, D. C., doi:10.1029/139GM07.

Schneider, D. J., W. I. Rose, and L. Kelley (1995), Tracking of 1992 eruption clouds from Crater Peak Vent of Mount Spurr Volcano, Alaska, using AVHRR, *U. S. Geol. Surv. Bull.*, *2139*, 27–36.

Schneider, D. J., W. Rose, L. Coke, G. Bluth, I. Sprod, and A. Krueger (1999), Early evolution of a stratospheric volcanic eruption cloud as observed with TOMS and AVHRR, *J. Geophys. Res.*, *104*, 4037–4050, doi:10.1029/1998JD200073.

Searcy, C., K. Dean, and W. Stringer (1998), PUFF: A high-resolution volcanic ash tracking model, *J. Volcanol. Geotherm. Res.*, *80*, 1–16, doi:10.1016/S0377-0273(97)00037-1.

Skamarock, W. C., J. B. Klemp, J. Dudhia, D. O. Gill, D. M. Barker, W. Wang, and J. G. Powers (2005), A description of the advanced research WRF version 2, *NCAR/TN-468+STR*, 8 pp., NCAR, Boulder, Colo.

Sparks, R. S. J., M. I. Bursik, S. N. Carey, J. S. Gilbert, L. S. Glaze, H. Sigurdsson, and A. W. Woods (1997), *Volcanic Plumes*, 574 pp., John Wiley, London.

Steensen, T., M. Stuefer, P. W. Webley, G. Grell, and S. Freitas (2012), Qualitative comparison of Mount Redoubt 2009 volcanic clouds using the PUFF and WRF-Chem dispersion models and satellite remote sensing data, *J. Volcanol. Geotherm. Res.*, doi:10.1016/j.jvolgeores.2012.02.018, in press.

Stohl, A., et al. (2011), Determination of time- and height-resolved volcanic ash emissions and their use for quantitative ash dispersion modeling: The 2010 Eyjafjallajökull eruption, *Atmos. Chem. Phys.*, *11*, 4333–4351, doi:10.5194/acp-11-4333-2011.

Suzuki, T. (1983), A Theoretical model for dispersion of tephra, in *Arc Volcanism: Physics and Tectonics*, edited by D. Shimozuru and I. Yokoyama, pp. 95–113, Terra Sci., Tokyo.

Webley, P. W., J. Dehn, J. Lovick, K. G. Dean, J. E. Bailey, and L. Valcic (2009a), Near real time volcanic ash cloud detection: Experiences from the Alaska Volcano Observatory, *J. Volcanol. Geotherm. Res.*, *186*(1–2), 79–90.

Webley, P. W., B. J. B. Stunder, and K. G. Dean (2009b), Significant eruption source parameter(s) for operational ash cloud transport and dispersion models, *J. Volcanol. Geotherm. Res.*, *186*(1–2), 108–119.

Wen, S., and W. I. Rose (1994), Retrievals of sizes and total masses of particles in volcanic clouds using AVHRR bands 4 and 5, *J. Geophys. Res.*, *99*(D3), 5421–5431, doi:10.1029/93JD03340.

Wiegner, M., J. Gasteiger, S. Groß, F. Schnell, V. Freudenthaler, and R. Forkel (2012), Characterization of the Eyjafjallajökull ash-plume: Potential of Lidar remote sensing, *J. Phys. Chem. Earth*, doi:10.1016/j.pce.2011.01.006, in press.

Winker, D. M. M., Z. Liu, A. H. Omar, J. Tackett, and T. D. D. Fairlie (2012), CALIOP observations of the transport of ash from the Eyjafjallajökull volcano in April 2010, *J. Geophys. Res.*, *117*, D00U15, doi:10.1029/2011JD016499.

Witham, C. S., M. C. Hort, R. Potts, R. Servranckx, P. Husson, and F. Bonnardot (2007), Comparison of VAAC atmospheric dispersion models using the 1 November 2004 Grímsvötn eruption, *Meteorol. Appl.*, *14*, 27–38, doi:10.1002/met.3.

World Meteorological Organization (WMO) (2010), Workshop on Ash Dispersal Forecast and Civil Aviation: Model definition document, report, 55 pp., Geneva, Switzerland. [Available at http://www.unige.ch/sciences/terre/mineral/CERG/Workshop/results/Model-Document-Geneva10.pdf.]

Yu, T., W. I. Rose, and A. J. Prata (2002), Atmospheric correction for satellite-based volcanic ash mapping and retrievals using "split window" IR data from GOES and AVHRR, *J. Geophys. Res.*, *107*(D16), 4311, doi:10.1029/2001JD000706.